

# Magnetorotational core-collapse supernovae.

**Sergey Moiseenko, Gennady Bisnovatyi-Kogan**

Space Research Institute,  
Moscow, Russia

# Outline

- Introduction
- Numerical method (implicit Lagrangian scheme)
- Magnetorotational(MR) mechanism of supernova explosion.
- Core-collapse simulations.
- MR supernova with quadrupole field.
- Magnetorotational instability(MRI) in MR supernova.
- MR supernova with dipole field, jet formation.
- MR supernova with different core masses and rotation rates.
- 3D features of MR supernova simulations
- Mirror symmetry violation of the magnetic field in rotating stars – one-sided jets, kicks.
- Conclusions.

# Introduction

## Supernova classification

- Type I – no hydrogen in SN spectra.
- Тип II – hydrogen lines in SN spectra.
- Type Ia – light curves are similar (thermonuclear supernovae)
- Type Ib – no hydrogen, but light curves resemble SN type II light curves.
- Type Ic – no helium lines, light curves resemble SN type II light curves.
- There is more detailed SN classification.

## Introduction (continued)

### Stars on late evolution stages. Gravitational collapse.

- Loss of stability. Averaged adiabatic index decrease  $5/3 \rightarrow 4/3$
- Iron dissociation.
- Collapse.
- Matter neutronization.
- Density in the center reaches nuclear values ( $2.8 \cdot 10^{14} \text{ g/sm}^3$ ).
- Neutrino cooling (URCA processes).
- The matter becomes nontransparent for neutrino.
- Formation of protoneutron star, radius 10-20 km.
- If the mass of the star  $> 30\text{-}40 M_{\text{sun}}$   $\rightarrow$  black hole can be formed.
- Supernova explosion  $\rightarrow$  star brightness increases by 9-10 orders.
- Maximal supernova luminosity  $\sim$  galaxy luminosity.
- Supernova explosion energy  $\sim 10^{51} \text{ erg}$ .

# Introduction (continued)

## Core collapse supernova explosions mechanisms

Spherically symmetrical model (neutrino deposition, shock wave formation).

(simulations by *Colgate, White; Ivanova, Imshennik, Nadezhin* ).

Shock stalls at 100-200km. No explosion.

Observations show: supernova explosions are asymmetrical (SN 1987A).

Neutrino convection and hydrodynamic instabilities:

Neutrino convection *inside protoneutron star* -> increase of the energy of radiated neutrino. Does not help to explosions.

Neutrino convection *after shock front* (detailed simulations does not lead to the supernova explosion *Mueller, Janka*)

**Standing Accretion Shock Instability (SASI)** (Blondin, Mezzacappa, Janka, Yamada...). Self-consistent simulations do not give explosion with sufficient level of confidence.

**Acoustic supernova** (Barrows) neutron star oscillations. Energy is too small for explosions. (papers by K.Sato group, our results)

**Magnetorotational supernova** (Bisnovatyi-Kogan, 1970). Rotation +magnetic field

# Operator-difference scheme

developed by N.V.Ardeljan et al. (Moscow State University)

Lagrangian, implicit, triangular grid with rezoning,  
completely conservative

Method of **basic** operators (Samarskii) – grid analogs of basic differential operators:

GRAD(scalar) (differential)  $\sim$  GRAD(scalar) (grid analog)

DIV(vector) (differential)  $\sim$  DIV(vector) (grid analog)

CURL(vector) (differential)  $\sim$  CURL(vector) (grid analog)

GRAD(vector) (differential)  $\sim$  GRAD(vector) (grid analog)

DIV(tensor) (differential)  $\sim$  DIV(tensor) (grid analog)

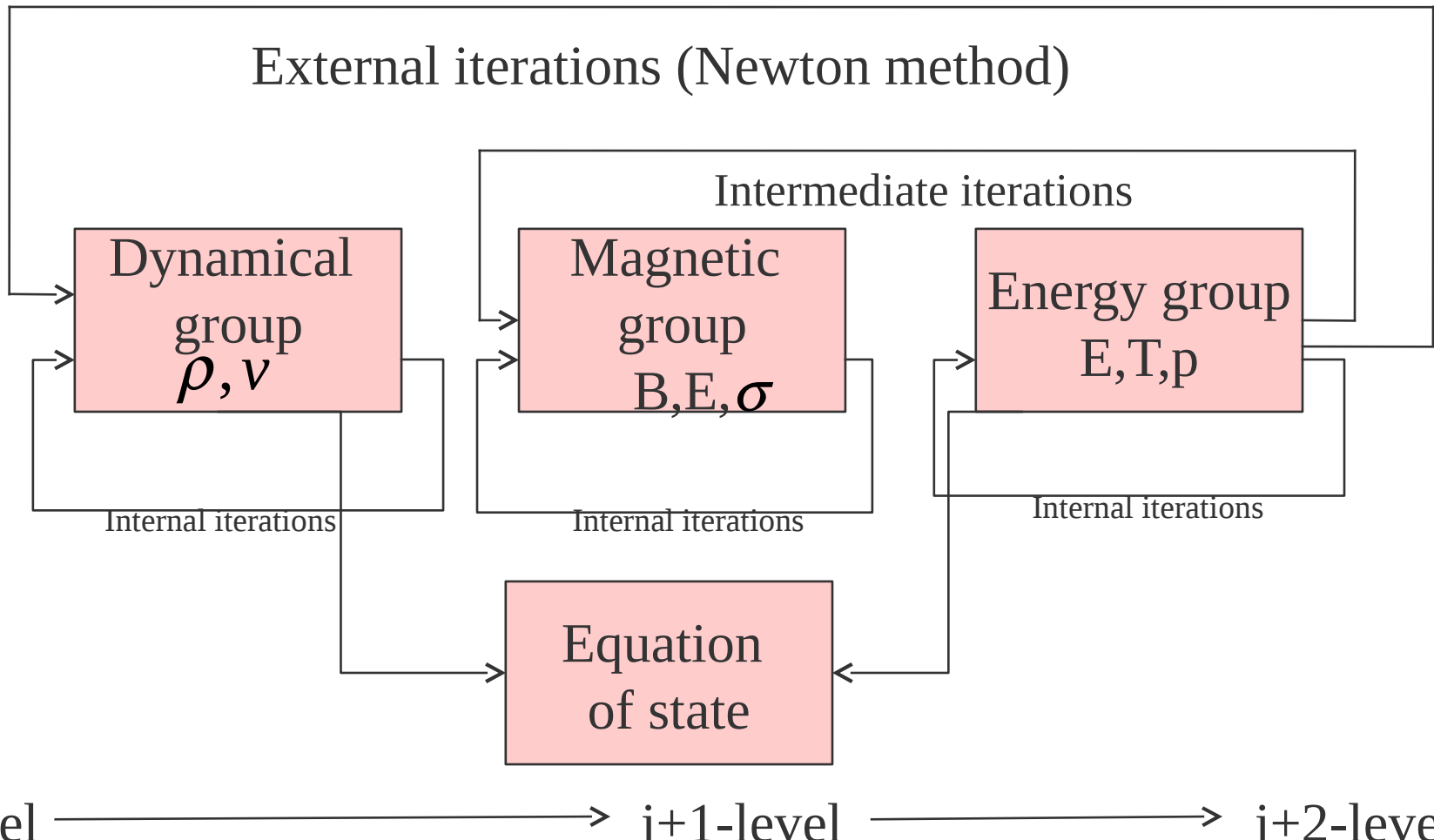
Implicit scheme. Time step restrictions are **weaker** for implicit schemes (no CFL condition).

The scheme is Lagrangian=> conservation of **angular** momentum.

*The stability of the method was explored in*

*Ardeljan & Kosmachevskii Comp. and Math. Modelling 1995, 6, 209 and references therein*

# General scheme for the IMPLICIT MHD numerical method

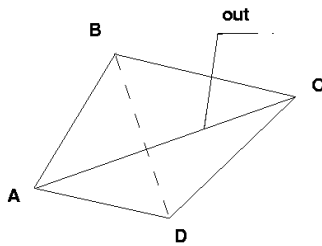


**j-level** → **j+1-level** → **j+2-level**

Operators are selfconjugated → Sparse matrices are symmetrical  
and positively defined

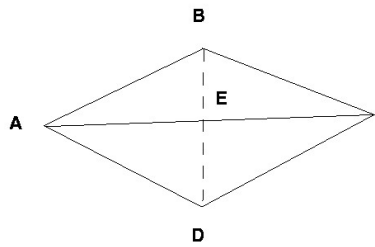
Matrices are inversed by conjugate gradients method (iterative).

# Grid reconstruction



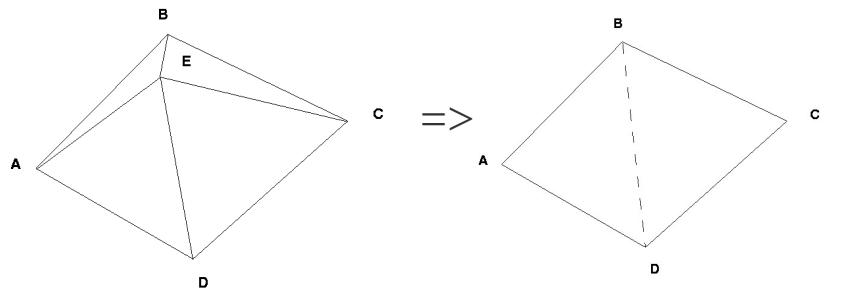
*Elementary reconstruction:* BD connection is introduced instead of AC connection. The total number of the knots and the cells in the grid is not changed.

---



*Addition a knot at the middle of the connection:*  
the knot E is added to the existing knots ABCD  
on the middle of the BD connection, 2 connections  
AE and EC appear and the total number of cells is  
increased by 2 cells.

---



*Removal a knot:* the knot E is removed from the grid  
and the total number of the cells is decreased by 2 cells

## Interpolation of grid functions on a new grid structure (local):

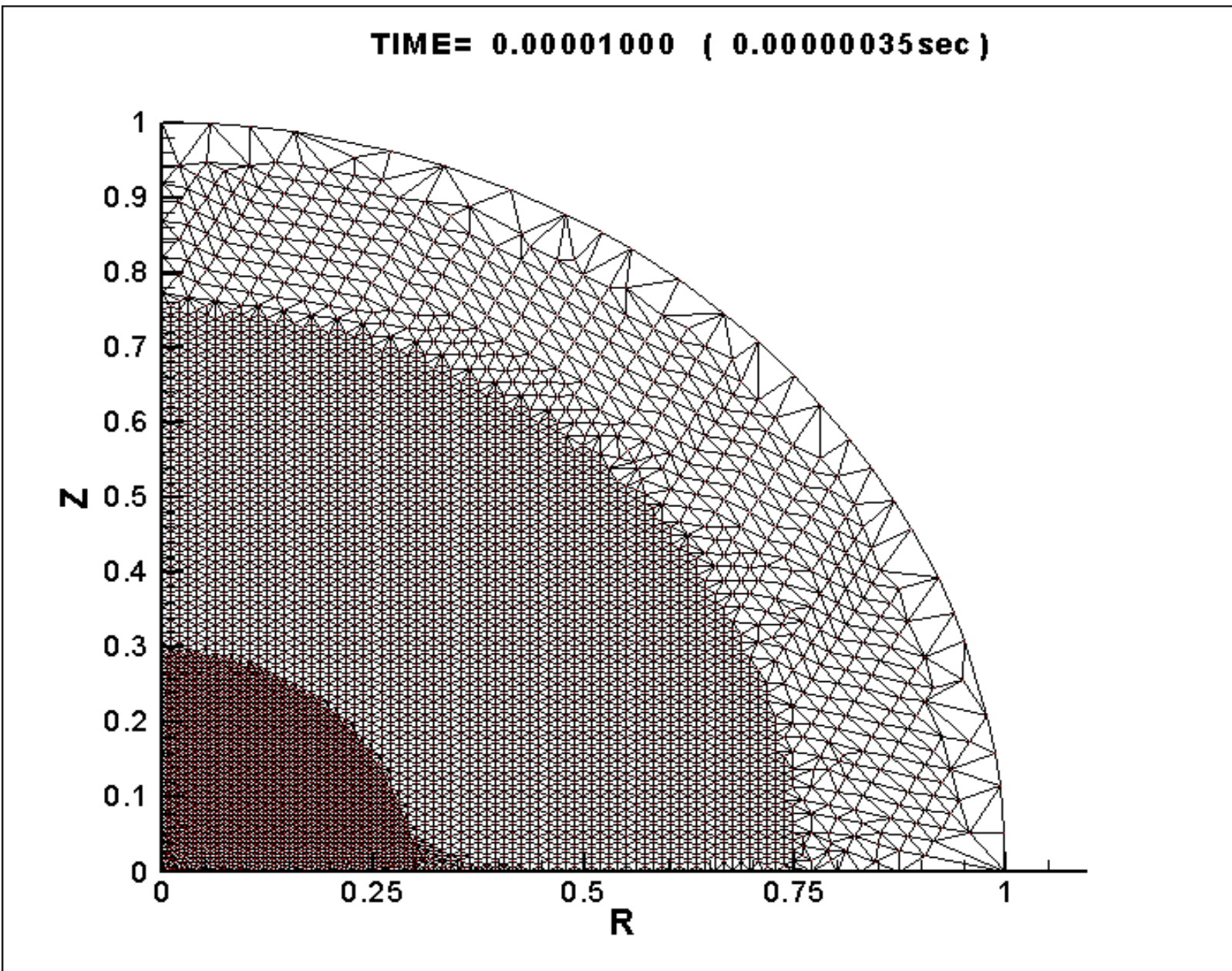
Should be made in *conservative* way. Conditional minimization of special functionals.

# Numerical method testing

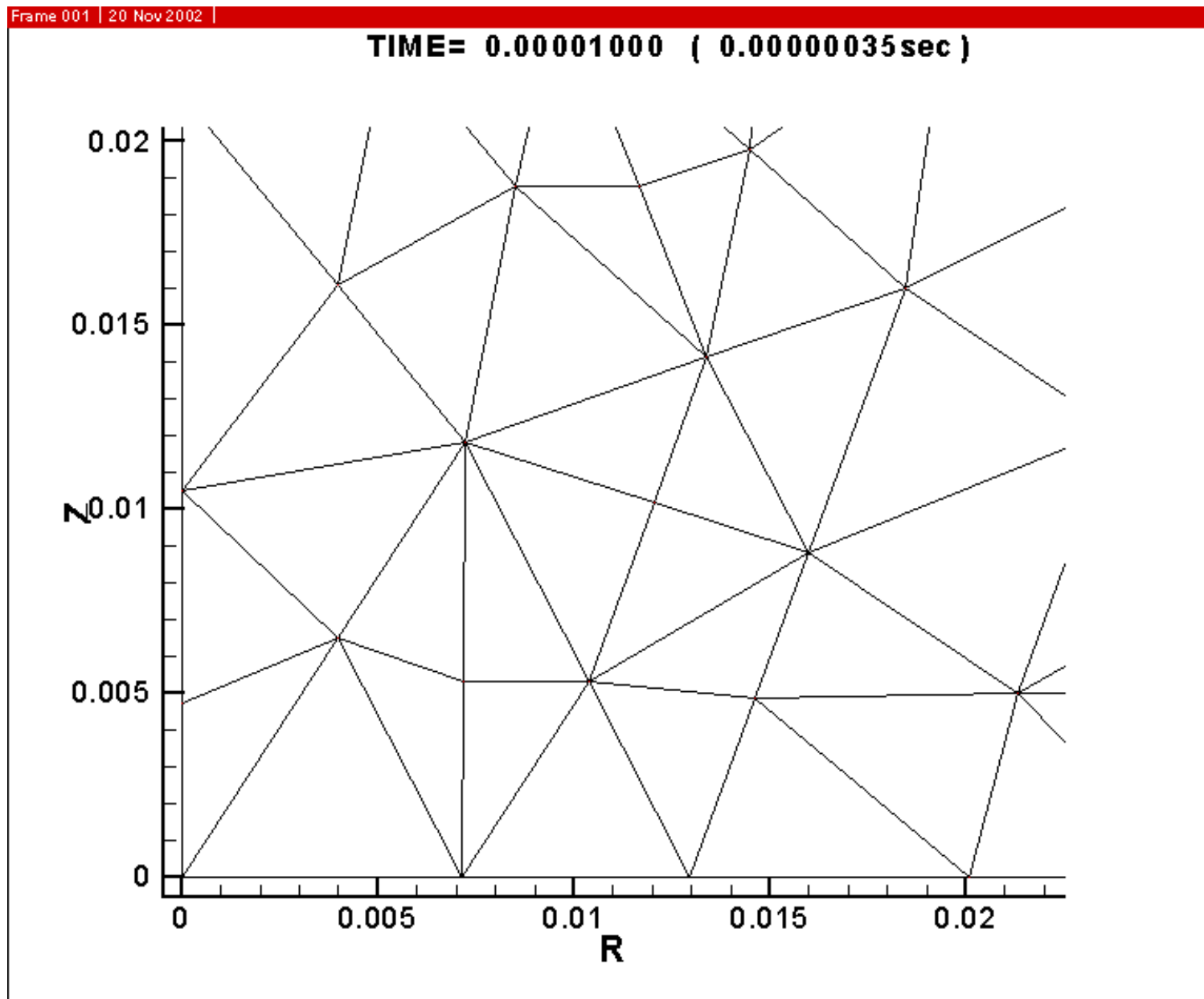
The method was tested on the following tests:

1. Collapse of a dust cloud without pressure
2. Decomposition of discontinuity problem
3. Spherical stationary solution with force-free magnetic field,
4. MHD piston problem,

## Example of calculation with the triangular grid

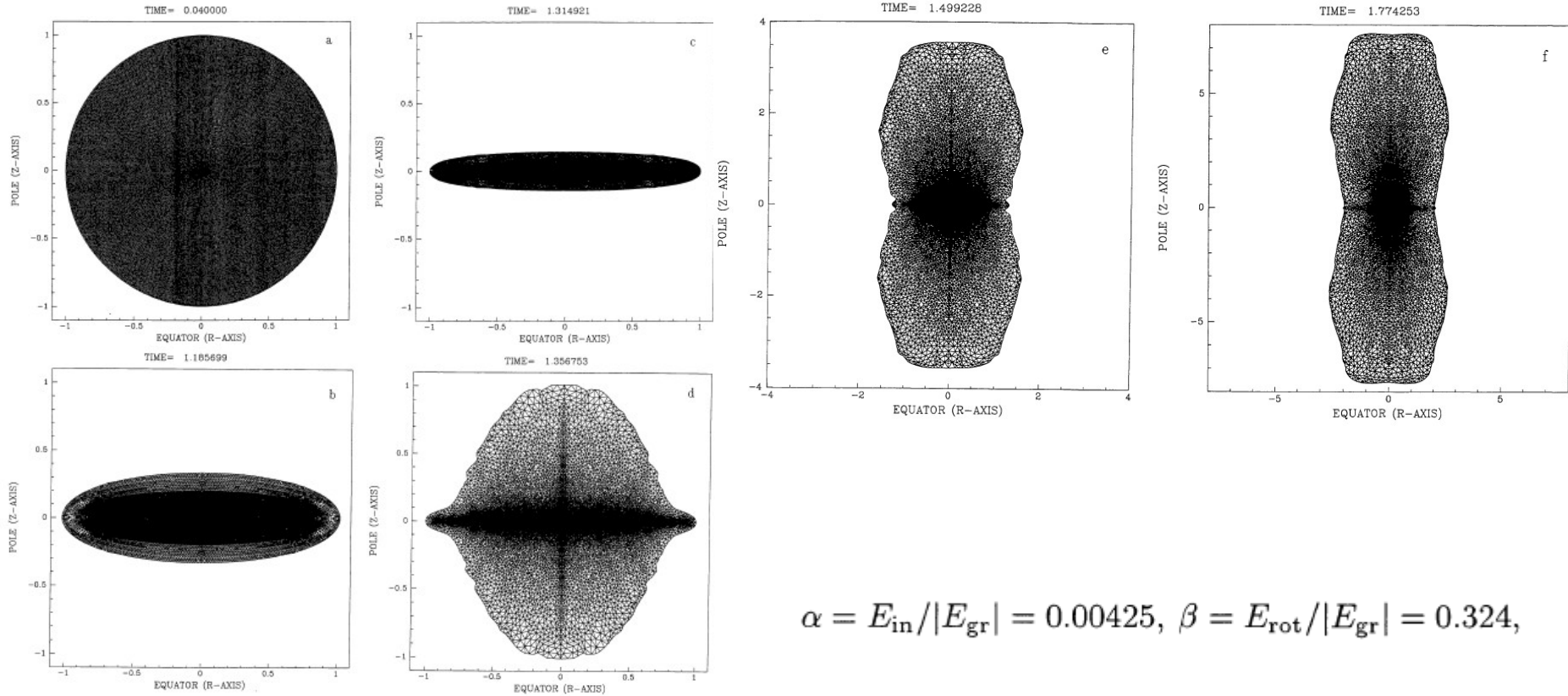


## Example of the triangular grid



# Collapse of rapidly rotating cold protostellar cloud

A&Ass 1996,115, 573



$$\alpha = E_{\text{in}}/|E_{\text{gr}}| = 0.00425, \beta = E_{\text{rot}}/|E_{\text{gr}}| = 0.324,$$

Magnetorotational mechanism for the supernova explosion Bisnovatyi-Kogan (1970)(original article was submitted: September 3, 1969)

Amplification of magnetic fields due to differential rotation, angular momentum transfer by magnetic field. Part of the rotational energy is transformed to the energy of explosion

First 2D calculations: LeBlanck&Wilson (1970 ) (original article was submitted: September 25, 1969) ->too large initial magnetic fields.  $E_{mag0} \sim E_{grav} \Rightarrow$  axial jet

Bisnovatyi-Kogan et al 1976, Meier et al. 1976, Ardeljan et al. 1979, Mueller & Hillebrandt 1979, Symbalisty 1984, Ardeljan et al. 2000, Wheeler et al. 2002, 2005, Yamada & Sawai 2004, Kotake et al. 2004, 2005, 2006, Burrows et al. 2007, Sawai, Kotake, Yamada 2008...

**It is popular topic now!**

The realistic values of the magnetic field are:  $E_{mag} \ll E_{grav}$  ( $E_{mag}/E_{grav} = 10^{-8}-10^{-12}$ )

Small initial magnetic field **-is the main difficulty** for the numerical simulations.

The hydrodynamic time scale is much smaller than the magnetic field amplification time scale (*if magnetorotational instability is neglected*).

Explicit difference schemes **can not** be applied. (CFL restriction on the time-step).

**Implicit schemes** should be used.

**Basic equations:** MHD +self-gravitation, infinite conductivity:

$$\begin{cases} \frac{dx}{dt} = \mathbf{u}, \frac{d\rho}{dt} + \rho \operatorname{div} \mathbf{u} = 0, \\ \rho \frac{du}{dt} = -\operatorname{grad} \left( p + \frac{\mathbf{H} \times \mathbf{H}}{8\pi} \right) + \frac{1}{4\pi} \operatorname{div}(\mathbf{H} \otimes \mathbf{H}) - \rho \operatorname{grad} \Phi \\ \rho \frac{d\varepsilon}{dt} + p \operatorname{div} \mathbf{u} + \rho F(\rho, T) = 0, p = P(\rho, T), \varepsilon = E(\rho, T), \\ \Delta \Phi = 4\pi G \rho, \\ \rho \frac{d}{dt} \left( \frac{\mathbf{H}}{\rho} \right) = \mathbf{H} \times \nabla \mathbf{u}. \end{cases} \quad \text{Additional condition } \operatorname{div} \mathbf{H} = 0$$

Axis symmetry ( $\frac{\partial}{\partial \phi} = 0$ ) and equatorial symmetry ( $z=0$ ) are supposed.

**Notations:**

$\frac{d}{dt} = \frac{\partial}{\partial t} + \mathbf{u} \times \nabla \mathbf{x}$  – velocity,  $\rho$  – density,  $p$  – pressure,

$\mathbf{H}$  – magnetic field,  $\Phi$  – gravitational potential,  $\varepsilon$  – internal energy,

$G$  – gravitational constant.

# Boundary conditions

Axial symmetry

$$r = 0 : u_r = u_\phi = H_r = H_\phi = \text{rot}_r \mathbf{H} = \text{rot}_\phi \mathbf{H} = 0,$$

---

Equatorial symmetry

$$u_z = H_z = 0, \quad \text{Quadrupole field}$$

$z = 0 :$       or

$$u_z = \frac{\partial B_z}{\partial z} = 0, \quad \text{Dipole field}$$

---

Outer boundary:  $P = \rho = T = H_\phi = 0, \mathbf{H}_{\text{poloidal}} = \mathbf{H}_q$

(from Biot-Savart law)

# Presupernova Core Collapse

Equations of state take into account degeneracy of electrons and neutrons, relativity for the electrons, nuclear transitions and nuclear interactions.

Temperature effects were taken into account approximately by the addition of radiation pressure and an ideal gas

.

Neutrino losses were taken into account in the energy equations.

A cool white dwarf was considered at the stability limit with a mass equal to the Chandrasekhar limit.

To obtain the collapse we increase the density at each point by 20% and we also impart uniform rotation on it.

## Equations of state (approximation of tables)

$$P \equiv P(\rho, T) = P_0(\rho) + \mathfrak{R}T\rho + \frac{T^4\sigma}{3}$$

$$P_0(\rho) = \begin{cases} P_0^{(1)} = b_1 \rho^{5/3} (1 + c_1 \rho^{1/3}), & \text{for } \rho \leq \rho_1 \\ P_0^{(k)} = a \cdot 10^{b_k (\lg \rho - 8.419)^{c_k}} & \text{for } \rho_{(k-1)} \leq \rho \leq \rho_k, k = 2, 6. \end{cases} \quad \varepsilon_0(\rho) = \int_0^\rho \frac{P_0(x)}{x^2} dx.$$

$$\varepsilon = \varepsilon(\rho, T) = \varepsilon_0(\rho) + \frac{3}{2} \mathfrak{R}T + \frac{\sigma T^4}{\rho} + \varepsilon_{Fe}(\rho, T), \quad \varepsilon_{Fe}(\rho, T) = \frac{E_{b,Fe}}{A_{m_p}} \left( \frac{T - T_{0,Fe}}{T_{1,Fe} - T_{0,Fe}} \right)^{\frac{1}{2}}, \quad \text{Fe-dis-sociation}$$

**Neutrino losses:** URCA processes, pair annihilation, photo production of neutrino, plasma neutrino

$$\text{URCA: } f(\rho, \bar{T}) = 1.3 \cdot 10^9 \chi(\bar{T}) / [1 + (7.1 \cdot 10^{-5} \rho / \bar{T}^3)^{2/5}] erg \cdot g^{-1} \cdot c^{-1}$$

$$\lambda(T) = \begin{cases} 1, \bar{T} < 7, \\ 664.31 + 51.024(\bar{T} - 20), 7 \leq \bar{T} \leq 20, \\ 664.31, \bar{T} > 20, \end{cases} \quad \bar{T} = T \cdot 10^{-9}.$$

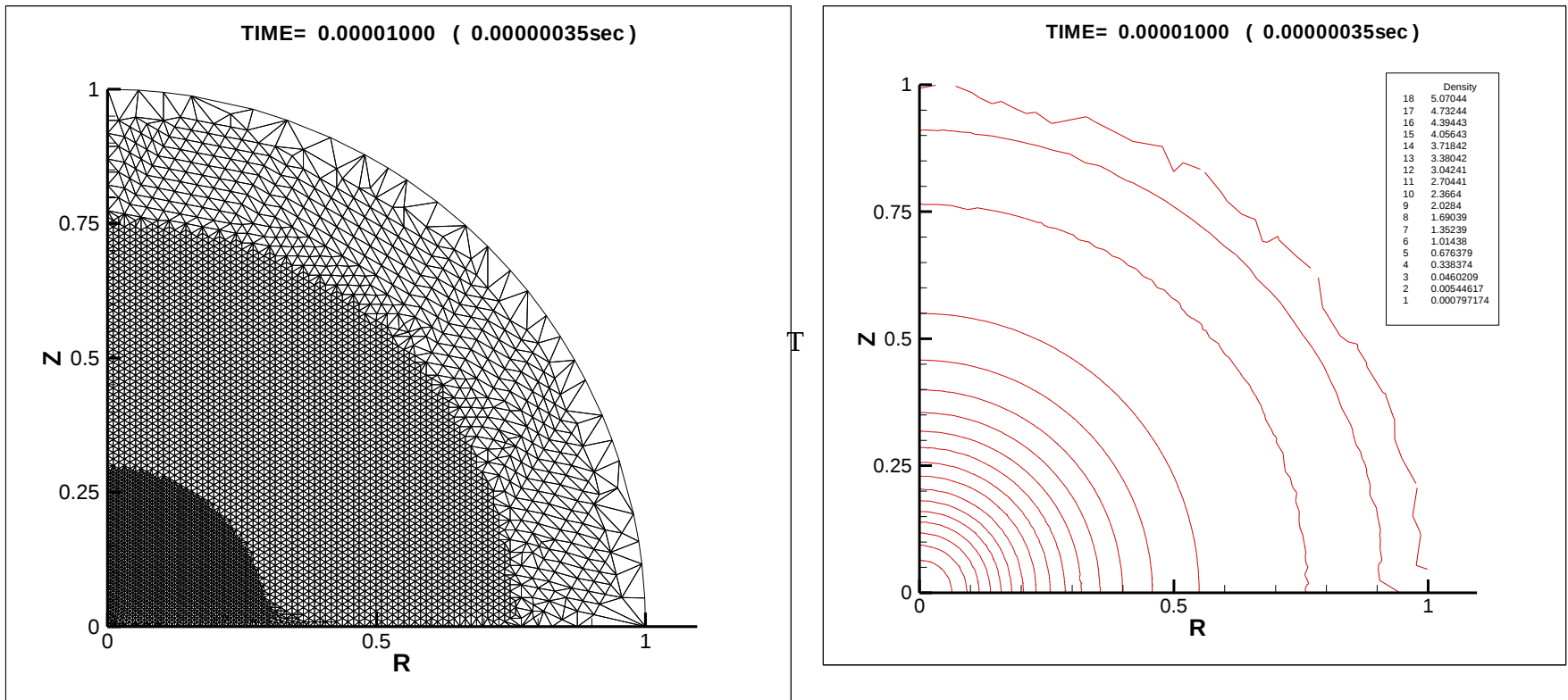
Approximation of tables from Ivanova, Imshennik, Nadyozhin, 1969

$$F(\rho, T) = f(\rho, T) e^{-\tau_\nu} \quad \text{neutrino diffusion}$$

## Initial state

$M = 1.2042 \times M_{sun}$ , spherically symmetrical stationary state, initial angular velocity 2.519 (1/sec)

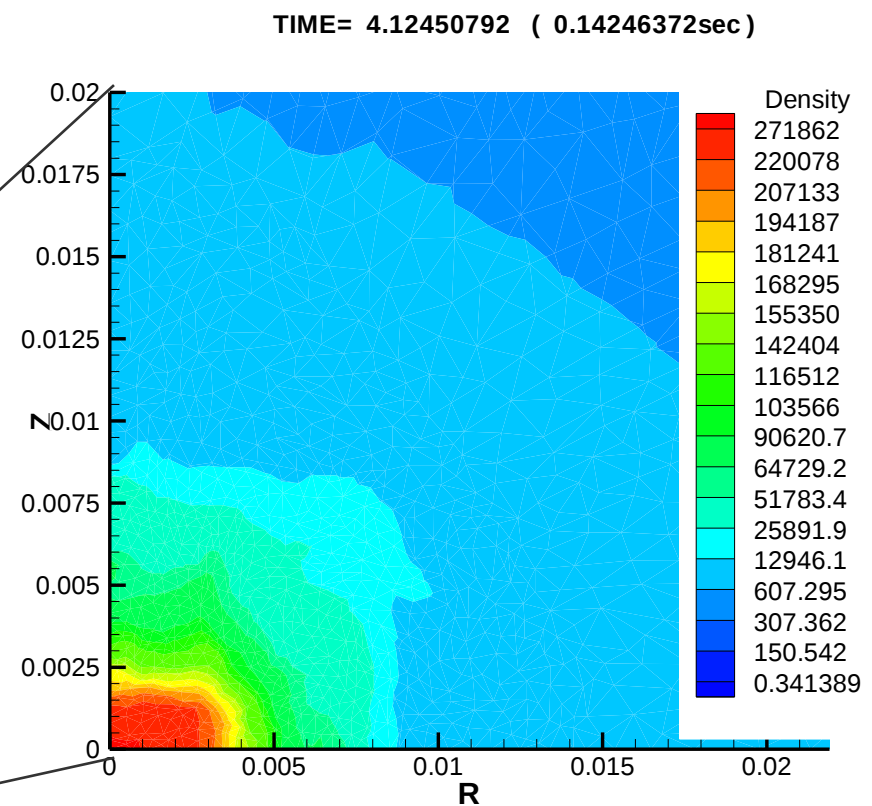
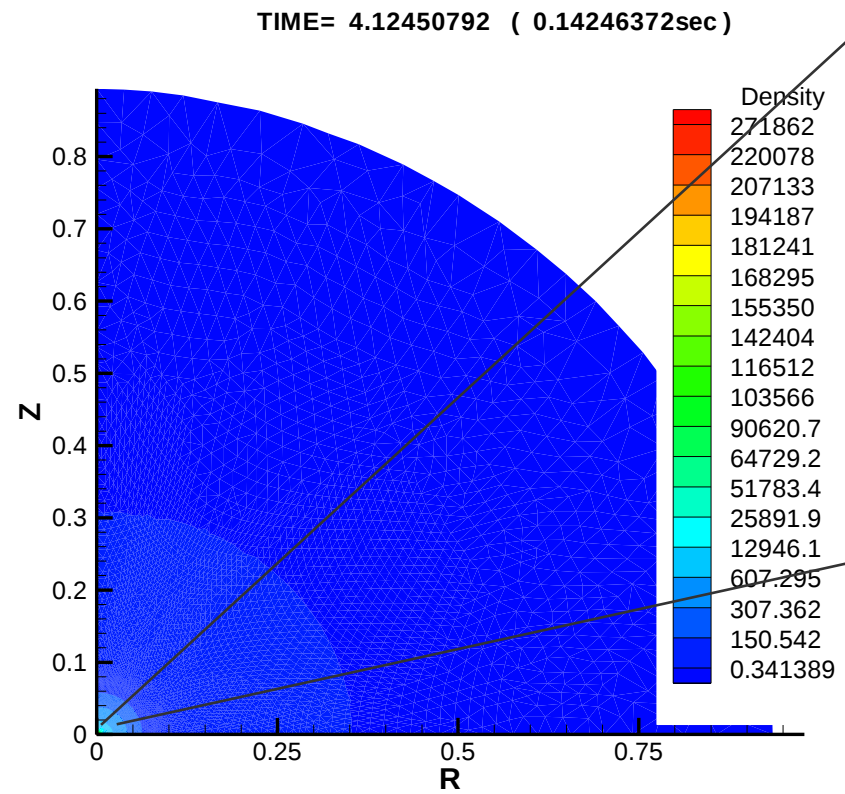
Initial temperature distribution  $T = \delta \rho^{2/3}$



$$\frac{E^{rot}}{E^{grav}} = 0.571\% \quad \frac{E^{int}}{E^{grav}} = 72.7\%$$

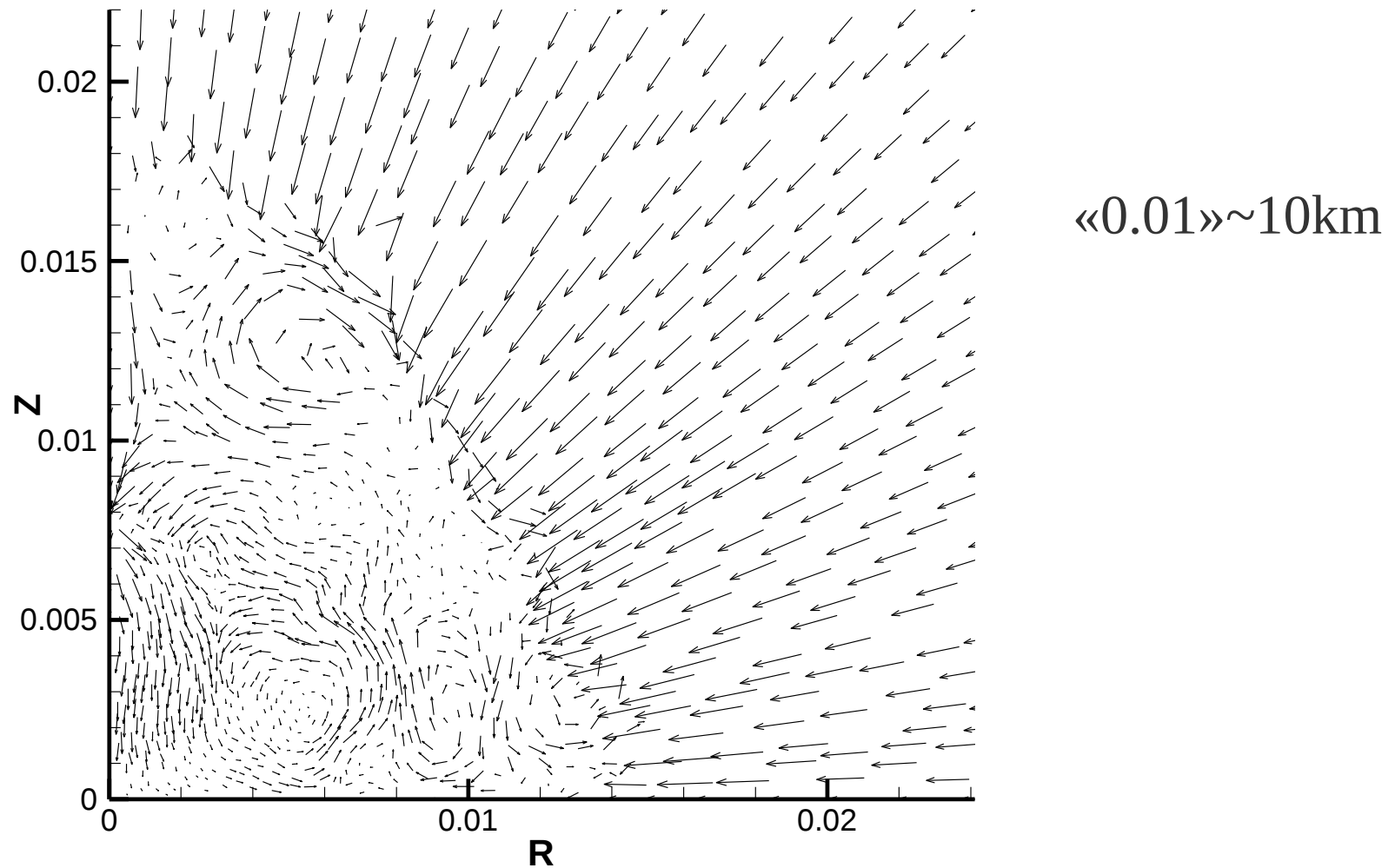
# Maximal compression state

Max. density =  $2.5 \cdot 10^{14} \text{ g/cm}^3$

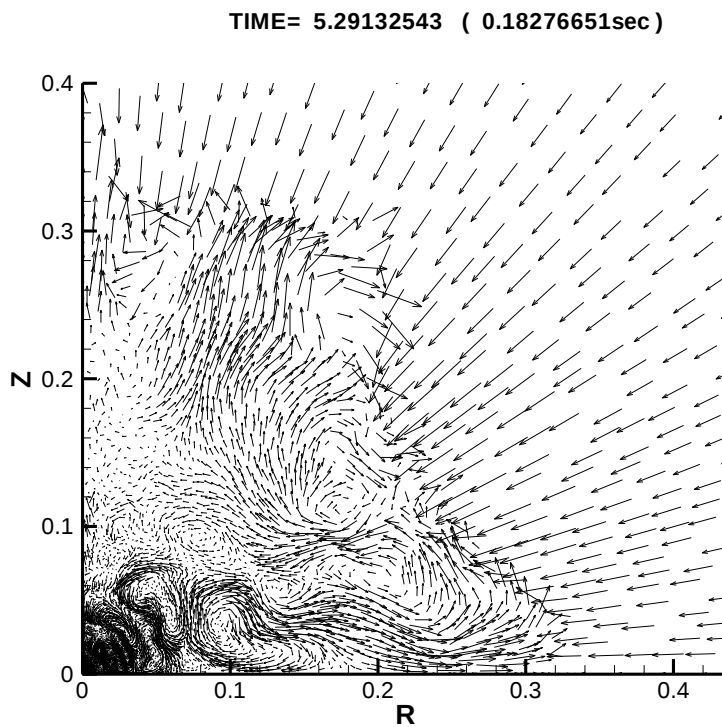
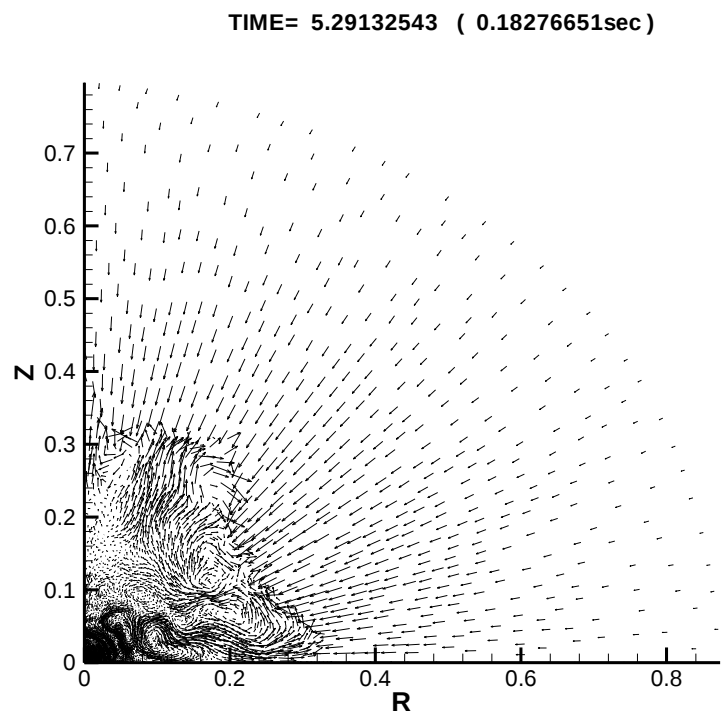


# Neutron star formation in the center and formation of the shock wave

TIME= 4.12450792 ( 0.14246372sec )



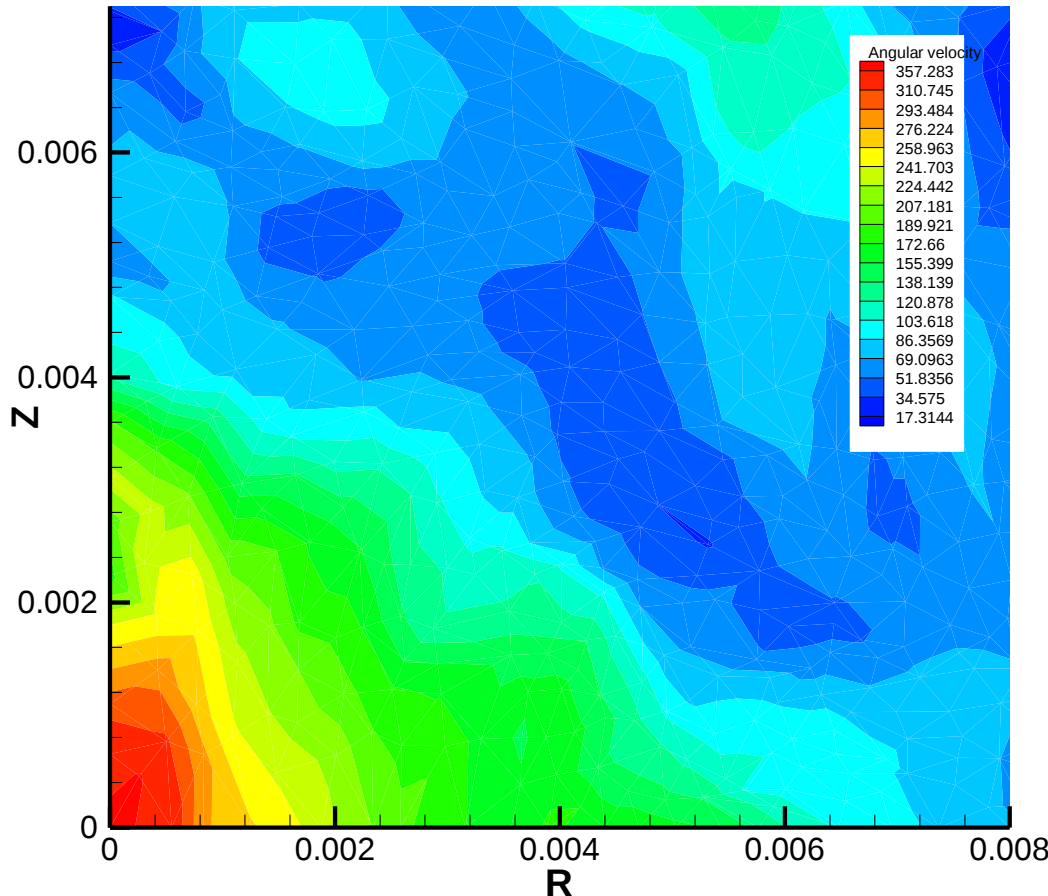
# Mixing



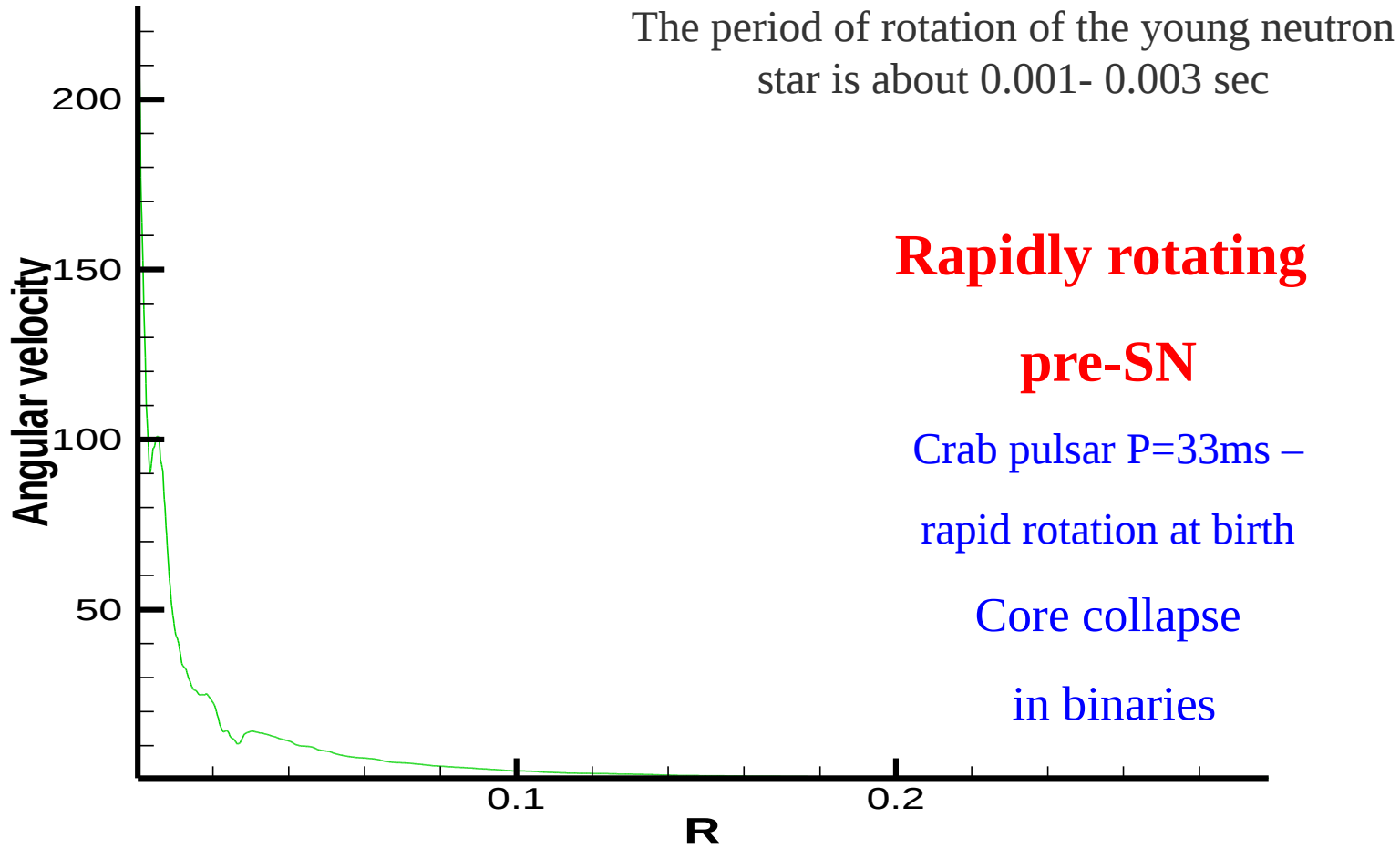
Bounce shock wave does not produce SN explosion :(

Angular velocity (central part of the computational domain). Rotation is **differential**.

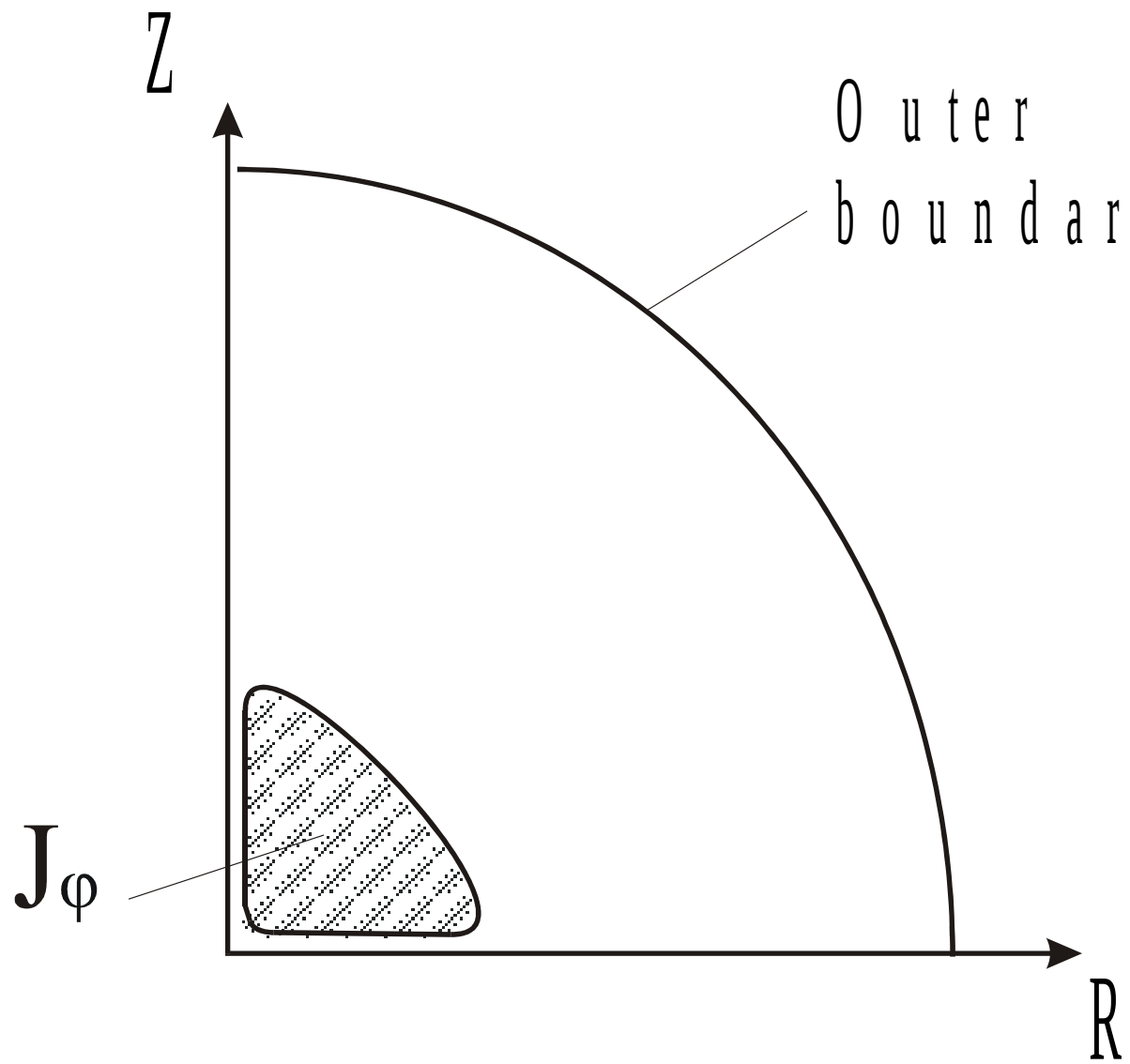
TIME= 4.15163360 ( 0.14340067 sec )



# Distribution of the angular velocity



# Initial magnetic field



Outer  
boundary

$$\mathbf{H} = \frac{1}{c} \int \frac{\mathbf{J} \times \mathbf{R}}{R^3} dv,$$

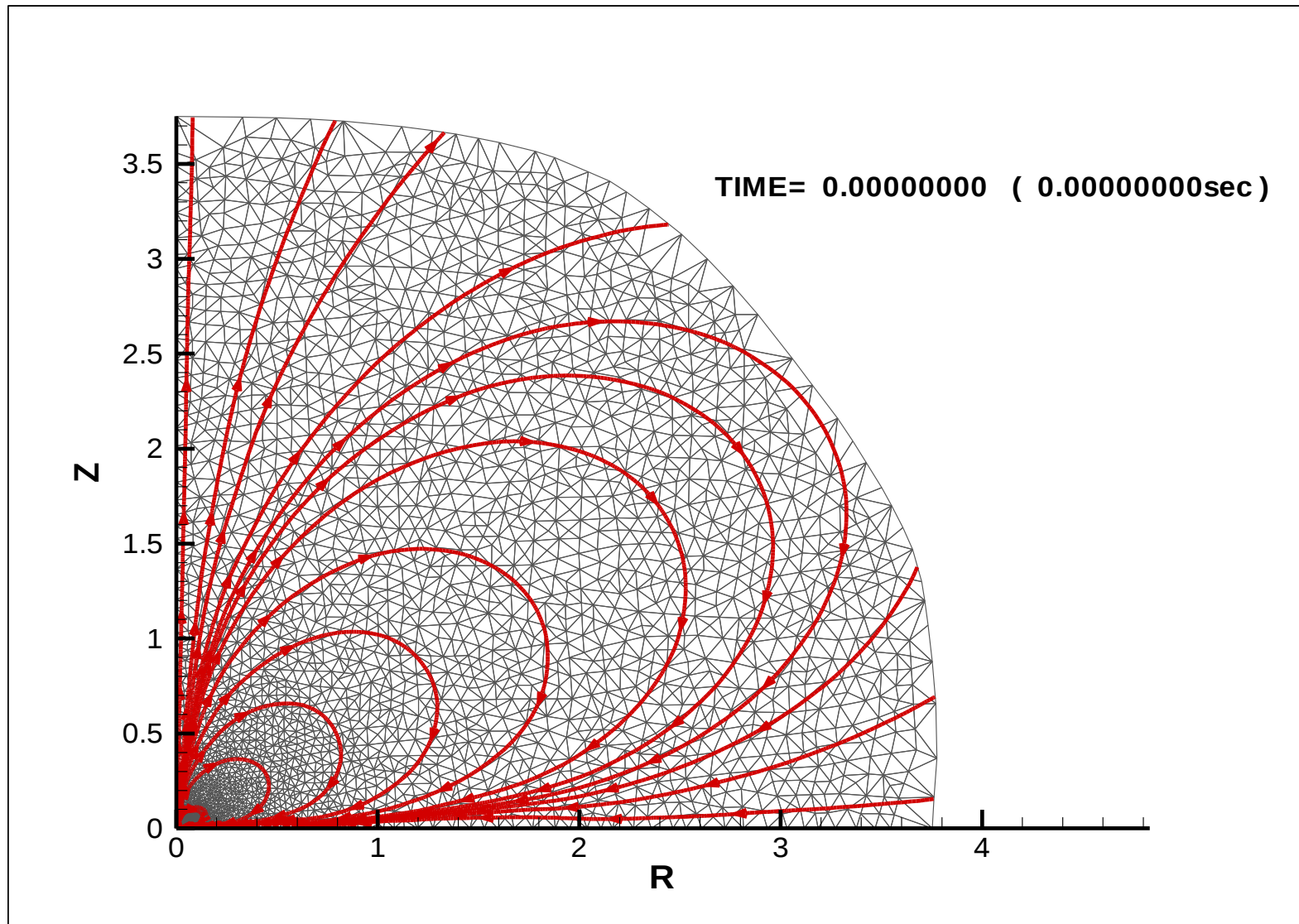
Biot-Savart law

$$J_\phi -> (H_r, H_z)$$

Initial poloidal  
magnetic field  
is divergence free,  
*BUT* not balanced. We  
have to balance it.

# Initial magnetic field –quadrupole-like symmetry

Ardeljan, Bisnovatyi-Kogan, SM, MNRAS 2005, 359, 333

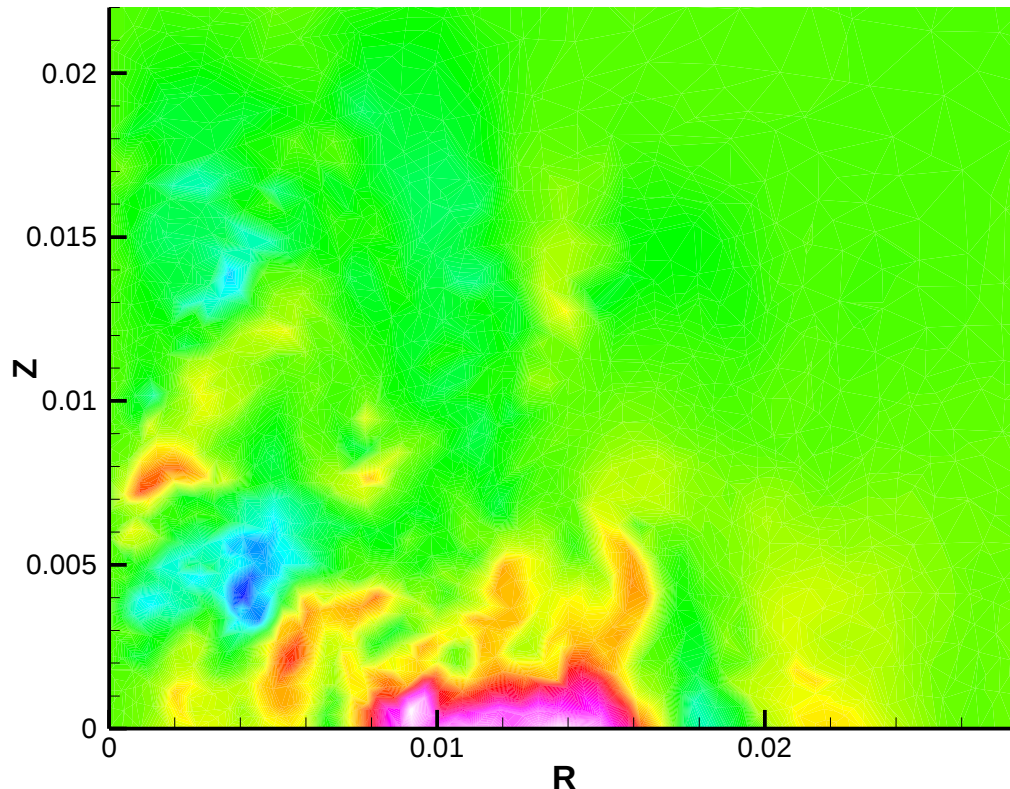


## Toroidal magnetic field amplification.

pink – maximum\_1 of  $Hf^2$     blue – maximum\_2 of  $Hf^2$

Maximal values of  $Hf = 2.5 \cdot 10^{16} G$

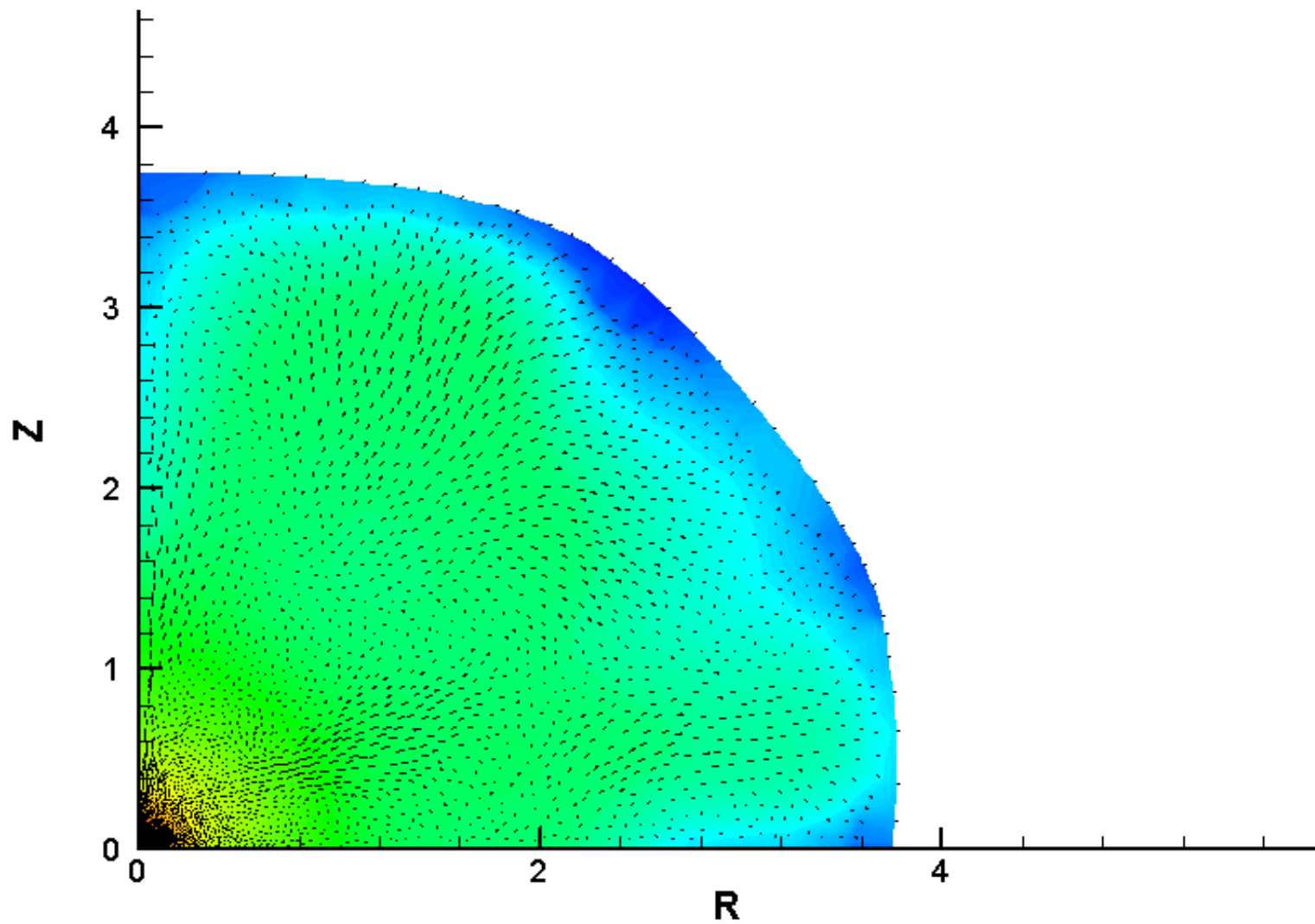
TIME= 0.00000779 ( 0.00000027 sec )



After SN explosion at the border of neutron star  $H = 2 \cdot 10^{14} G$

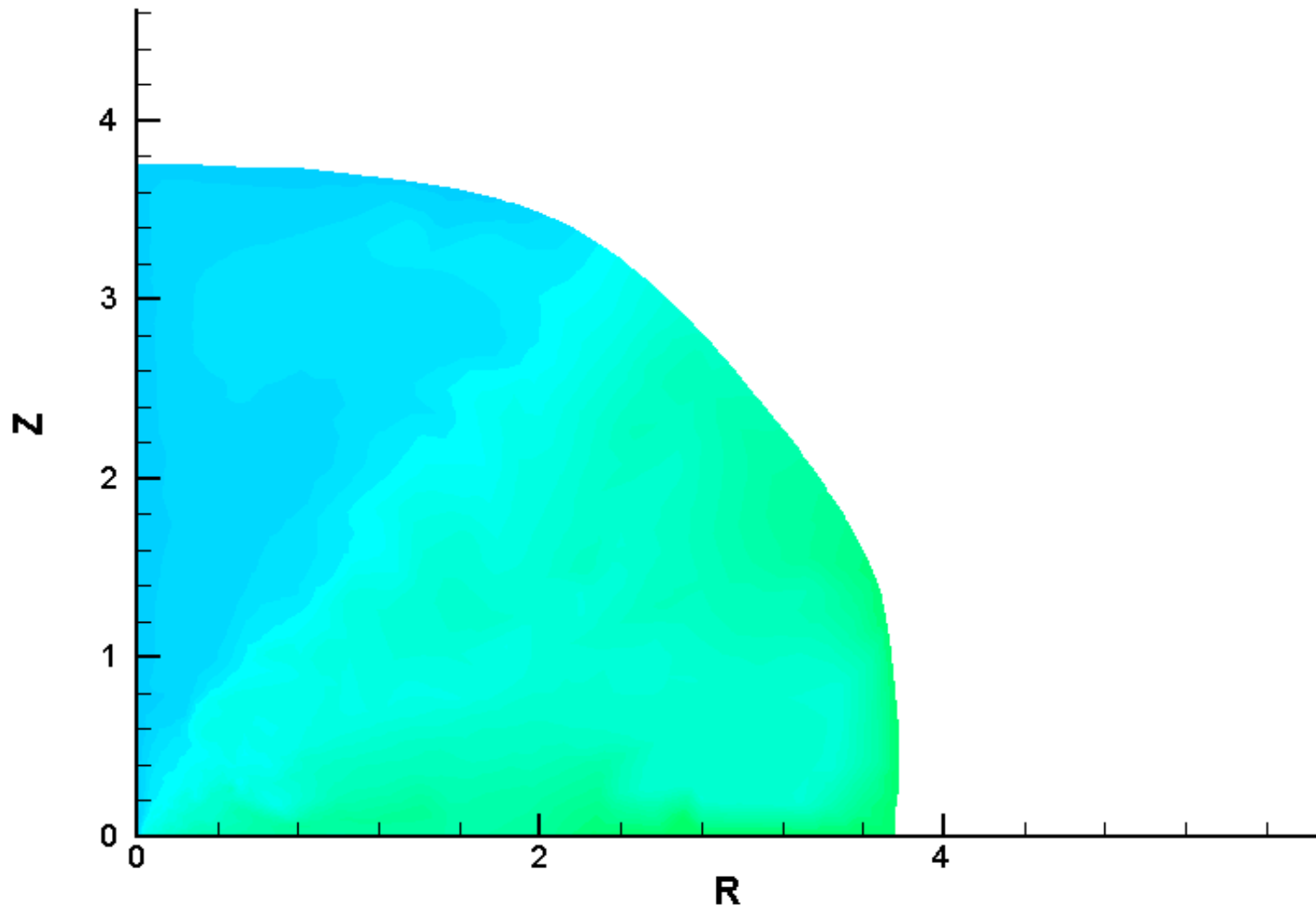
# Temperature and velocity field

**TIME= 0.00000779 ( 0.00000027 sec )**

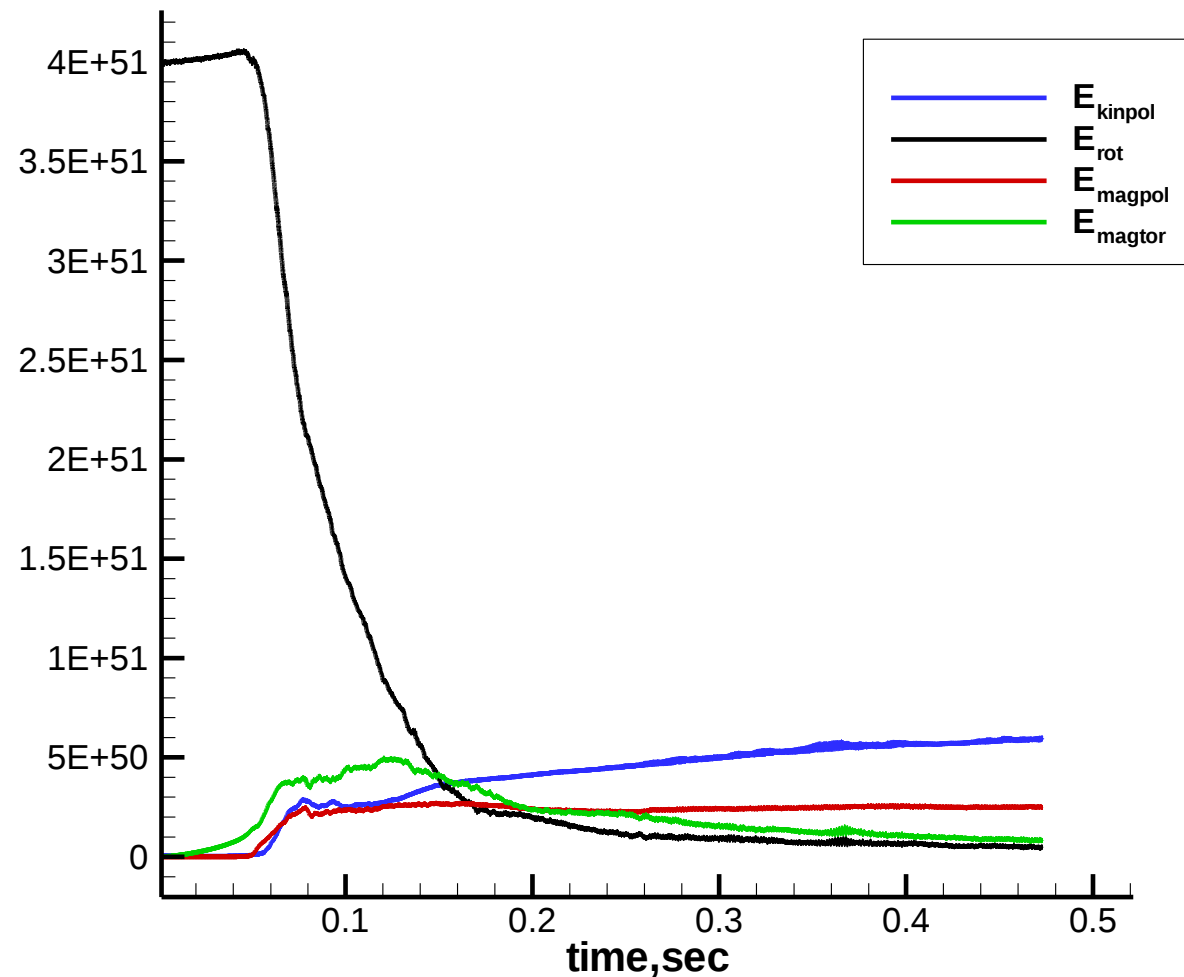


# Specific angular momentum $rV_\phi$

TIME= 0.00000779 ( 0.00000027 sec )

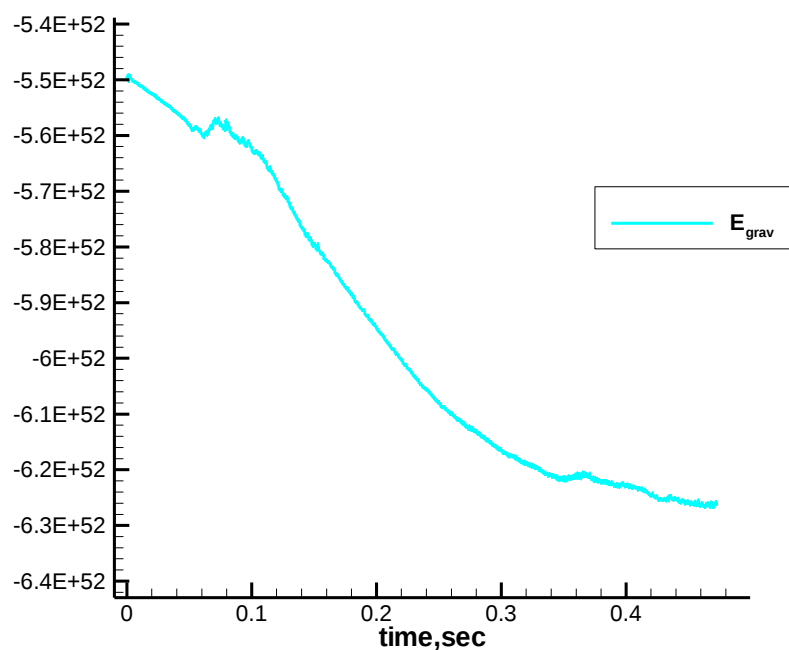


## Time evolution of different types of energies

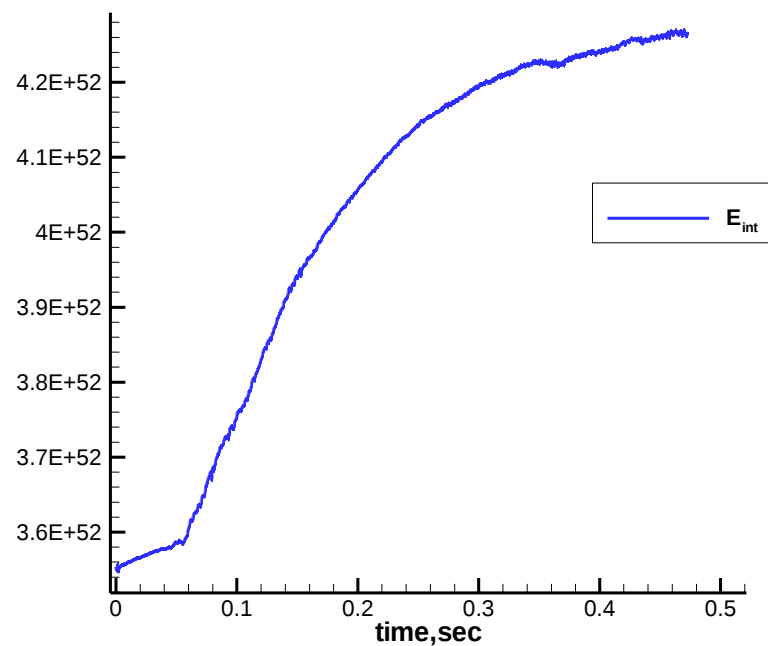


# Time evolution of the energies

Gravitational energy

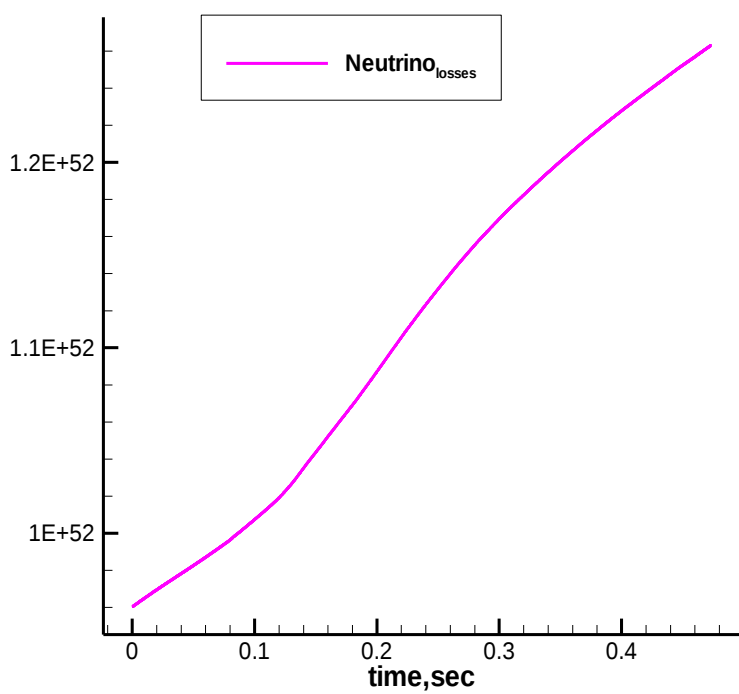


Internal energy

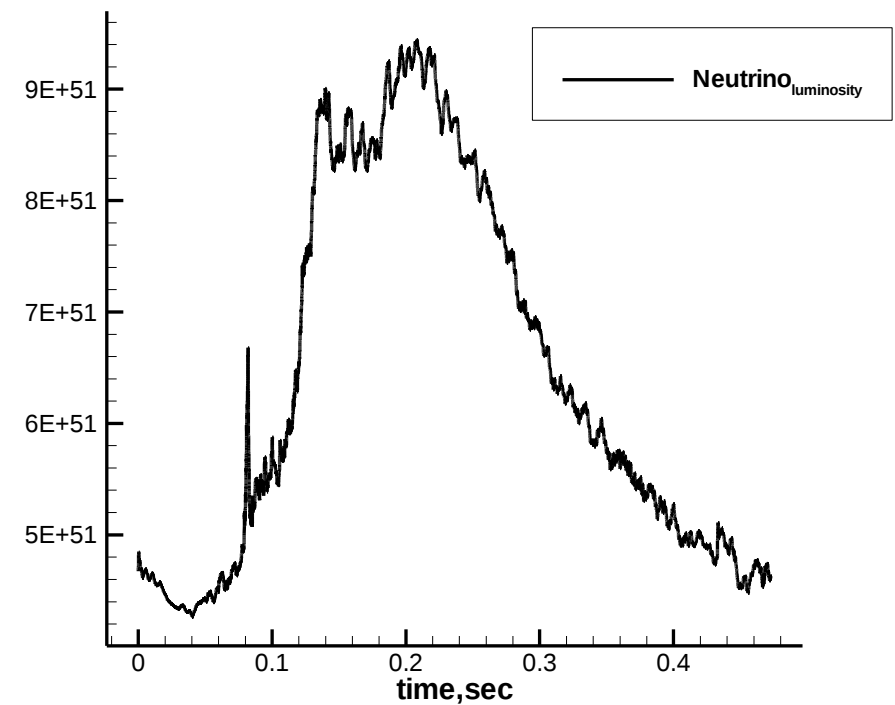


## Time evolution of the energies

Neutrino losses (ergs)



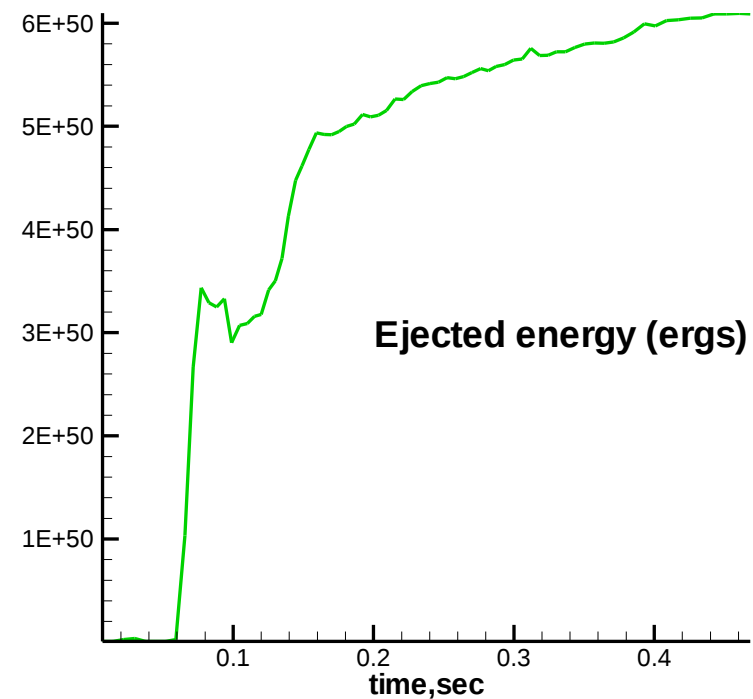
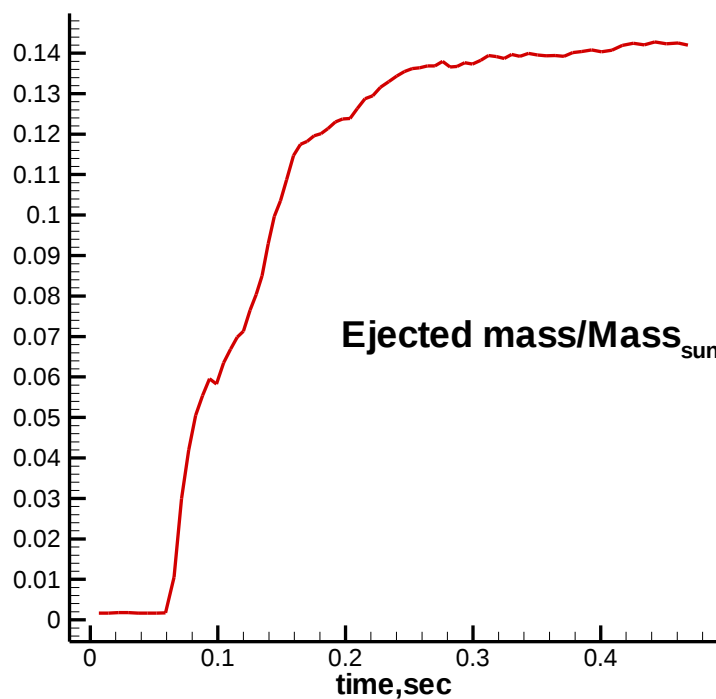
Neutrino luminosity (ergs/sec)



## Ejected energy and mass

Ejected energy  $0.6 \times 10^{51} erg$       Ejected mass  $0.14 M_{\odot}$

Particle is considered “ejected” –  
if its kinetic energy is greater than its potential energy



# Magnetorotational supernova in 1D

Bisnovaty-Kogan et al. 1976, Ardeljan et al. 1979

$$t_{\text{explosion}} : \frac{1}{\sqrt{\alpha}}, \quad \left( \alpha = \frac{E_{\text{mag}0}}{E_{\text{grav}0}} \right)$$

Example:  $\alpha = 10^{-2} \Rightarrow t_{\text{explosion}} = 10,$

$\alpha = 10^{-12} \Rightarrow t_{\text{explosion}} = 10^6 !!!$

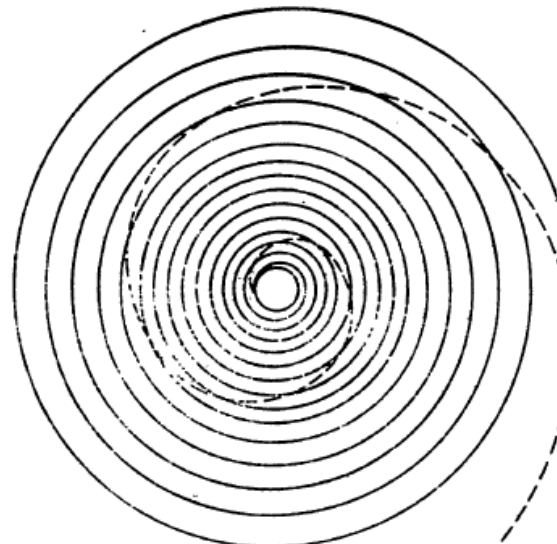
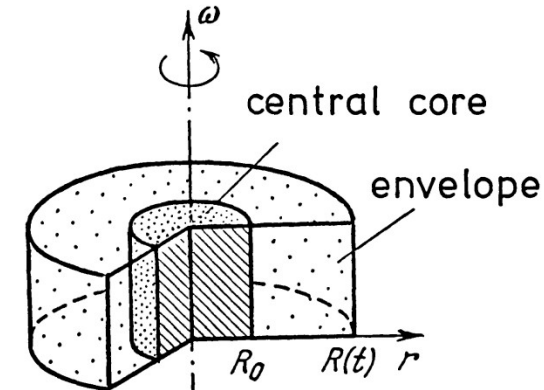
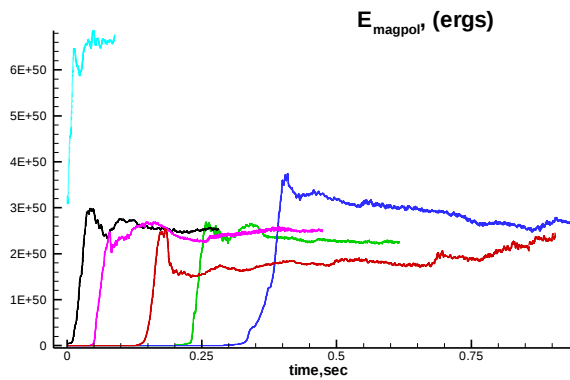
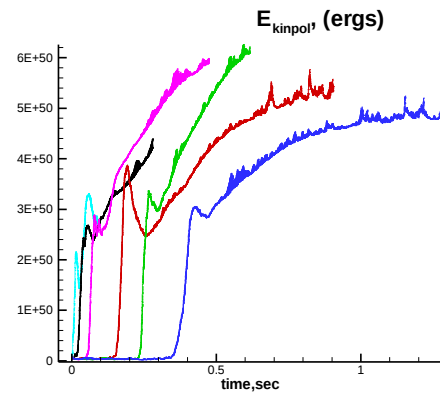
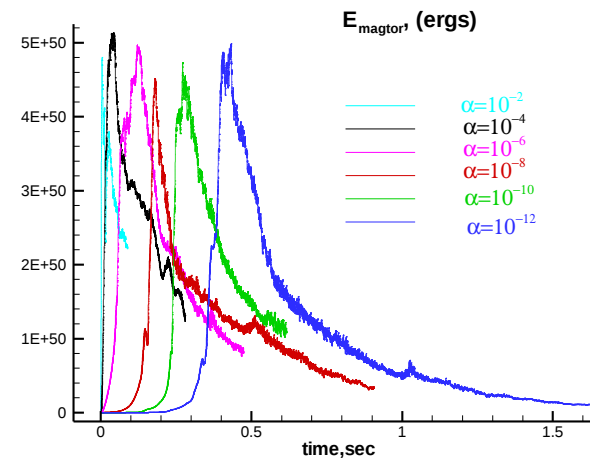
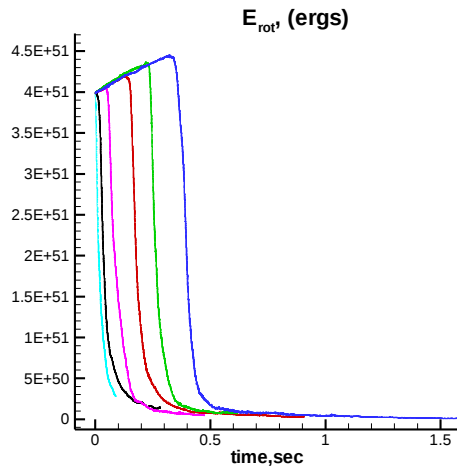


FIG. 3. Shape of a field line in the region near the core at the time  $t_\alpha = 7$  for  $\alpha = 10^{-2}$  (dashed line) and  $\alpha = 10^{-4}$  (solid line).

Magnetorotational explosion for the different  $\alpha = \frac{E_{mag0}}{E_{grav0}} = 10^{-2} - 10^{-12}$

Magnetorotational instability [ mag. field grows exponentially  
 (Dungey 1958, Velikhov 1959, Chandrasekhar, Balbus & Hawley 1991,  
 Spruit 2002, Akiyama et al. 2003...)]



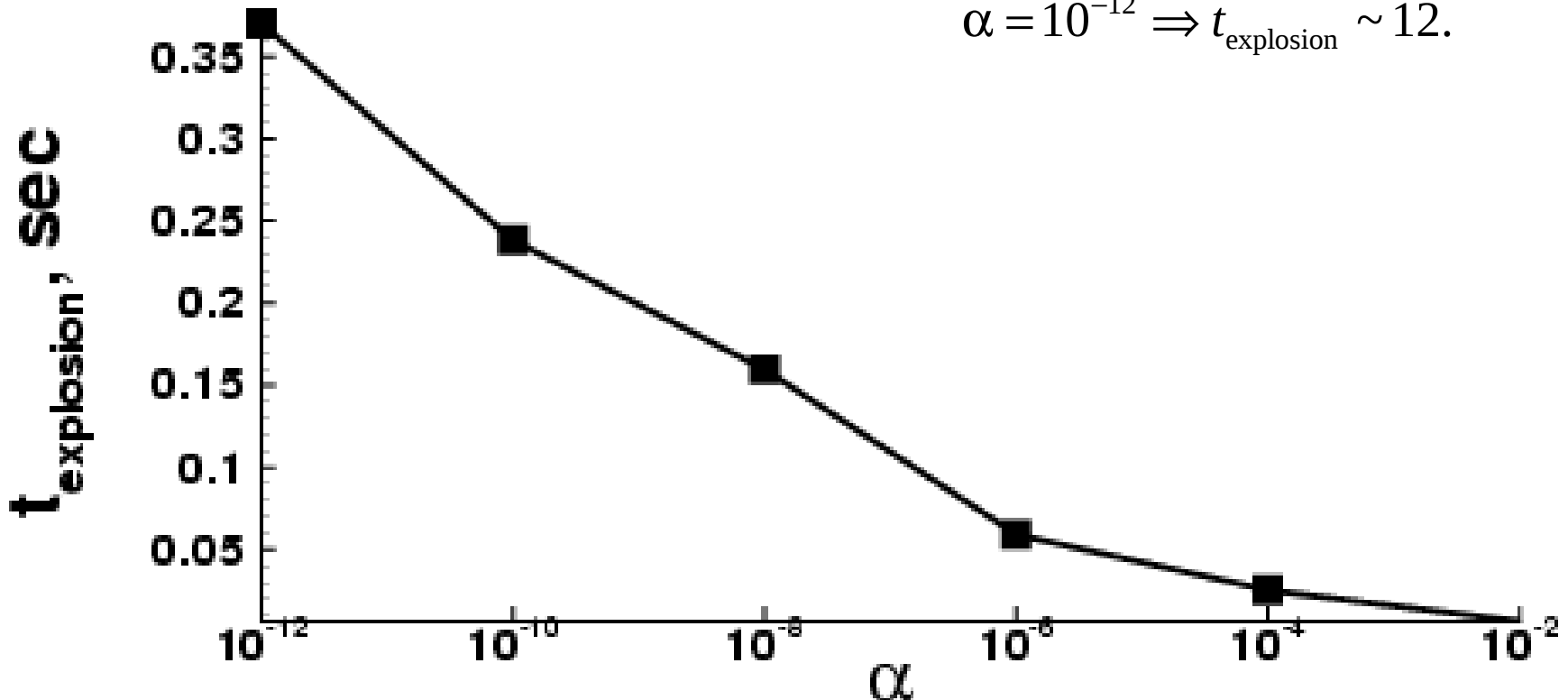
Dependence of the explosion time from  $\alpha = \frac{E_{\text{mag}0}}{E_{\text{grav}0}}$

$$t_{\text{explosion}} \sim -\log(\alpha) \quad (\text{for small } \alpha)$$

$$\alpha = 10^{-6} \Rightarrow t_{\text{explosion}} \sim 6,$$

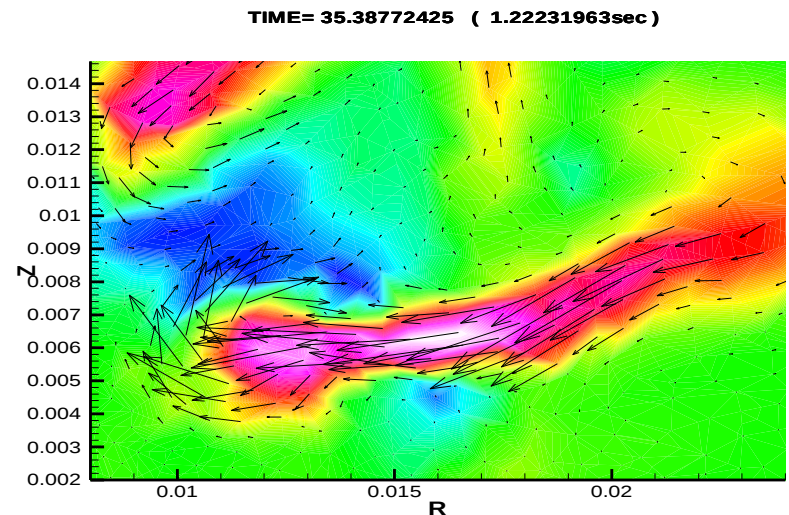
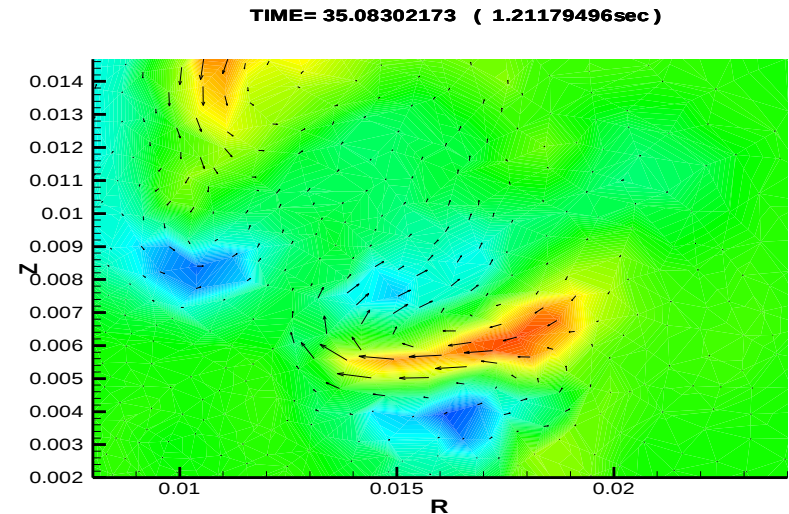
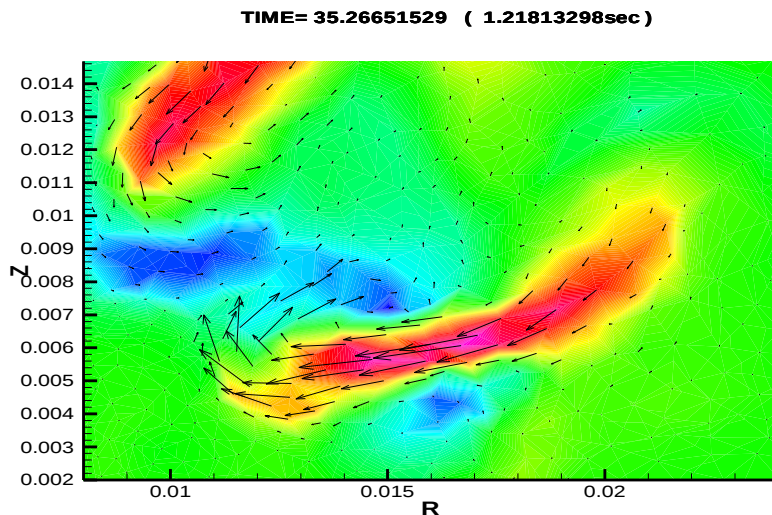
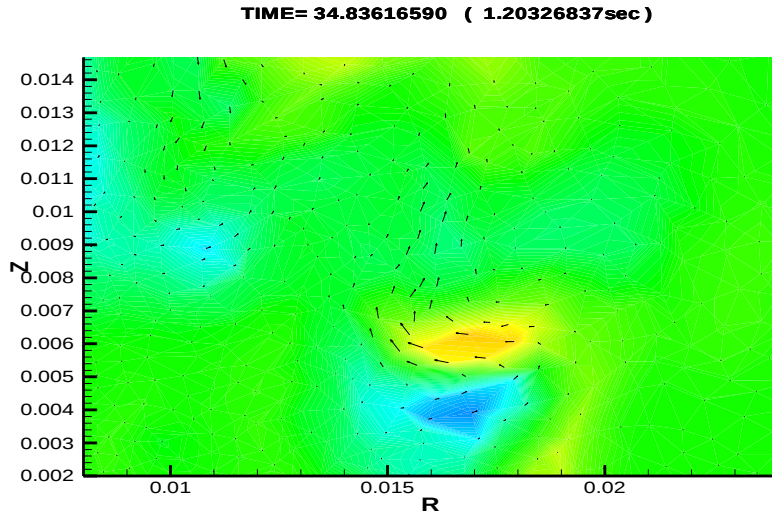
Example:

$$\alpha = 10^{-12} \Rightarrow t_{\text{explosion}} \sim 12.$$



# Magnetorotational instability

Central part of the computational domain . Formation of the MRI.



## Toy model for MRI in the magnetorotational supernova

$$\frac{dH_\varphi}{dt} = H_r \left( r \frac{d\Omega}{dr} \right); \quad \text{at the initial stage of the process } H_\varphi < H_\varphi^* : H_r \left( r \frac{d\Omega}{dr} \right) \approx \text{const},$$

beginning of the MRI  $\Rightarrow$  formation of multiple *poloidal* differentially rotating

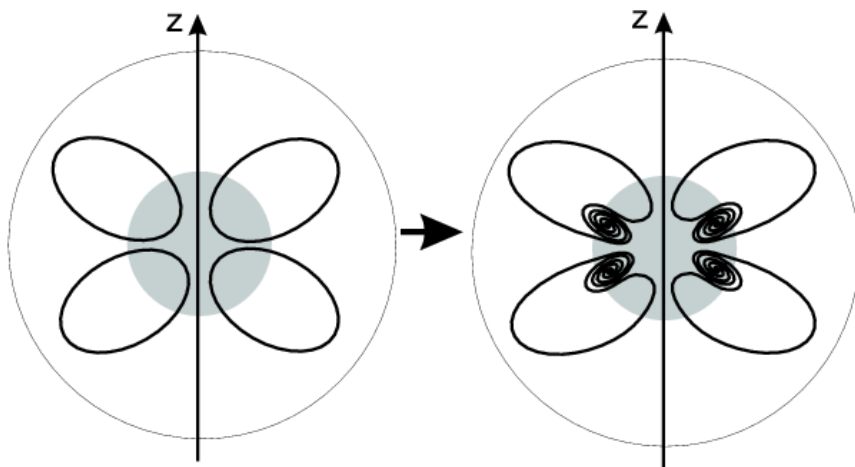
vortexes  $\frac{dH_r}{dt} = H_{r0} \left( \frac{d\omega_v}{dl} \right)$ , in general we may approximate:  $\left( \frac{d\omega_v}{dl} \right) \approx \alpha (H_\varphi - H_\varphi^*)$ .

Assuming for the simplicity that  $(r \frac{d\Omega}{dr}) = A$  is a constant during the first stages of MRI, and taking  $H_\varphi^*$  as a constant we come to the following equation:

$$\frac{d^2}{dt^2} (H_\varphi - H_\varphi^*) = AH_{r0}\alpha(H_\varphi - H_\varphi^*)$$

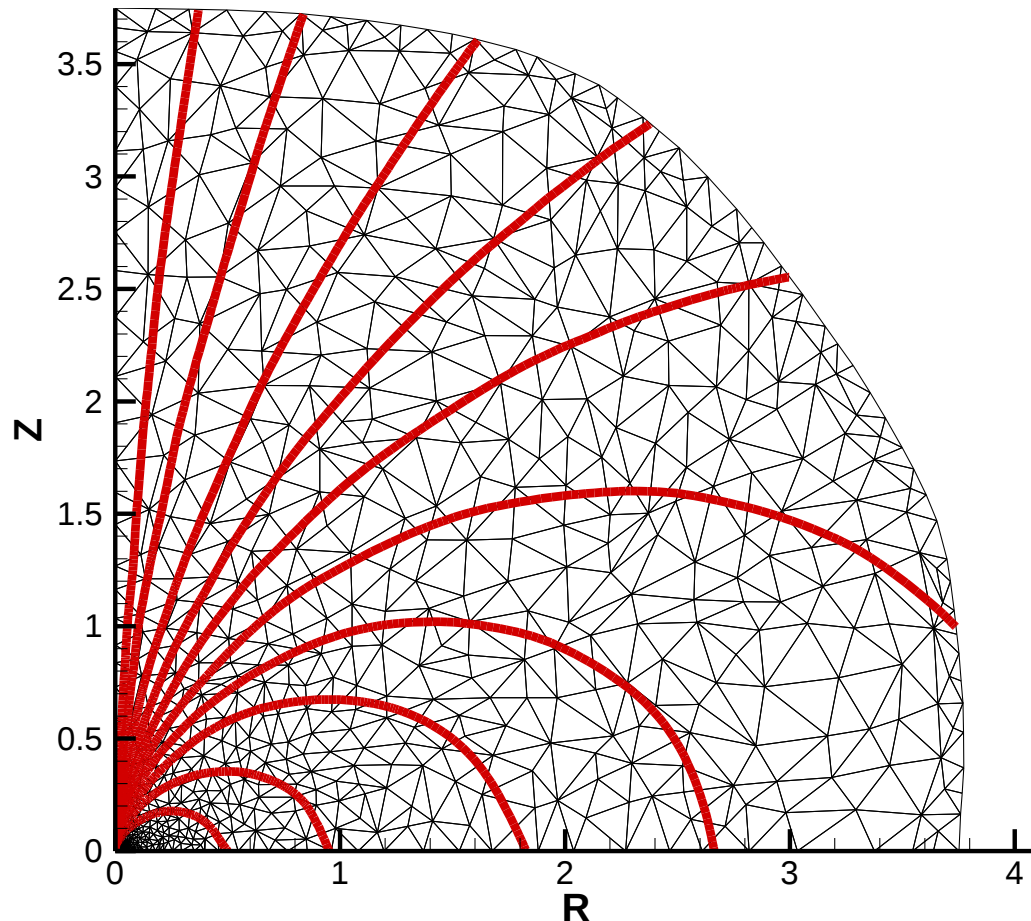


$$\begin{cases} H_\varphi = H_\varphi^* + H_{r0} e^{\sqrt{A\alpha H_{r0}}(t-t^*)}, \\ H_r = H_{r0} + \frac{H_{r0}^{3/2} \alpha^{1/2}}{\sqrt{A}} \left( e^{\sqrt{A\alpha H_{r0}}(t-t^*)} - 1 \right). \end{cases}$$

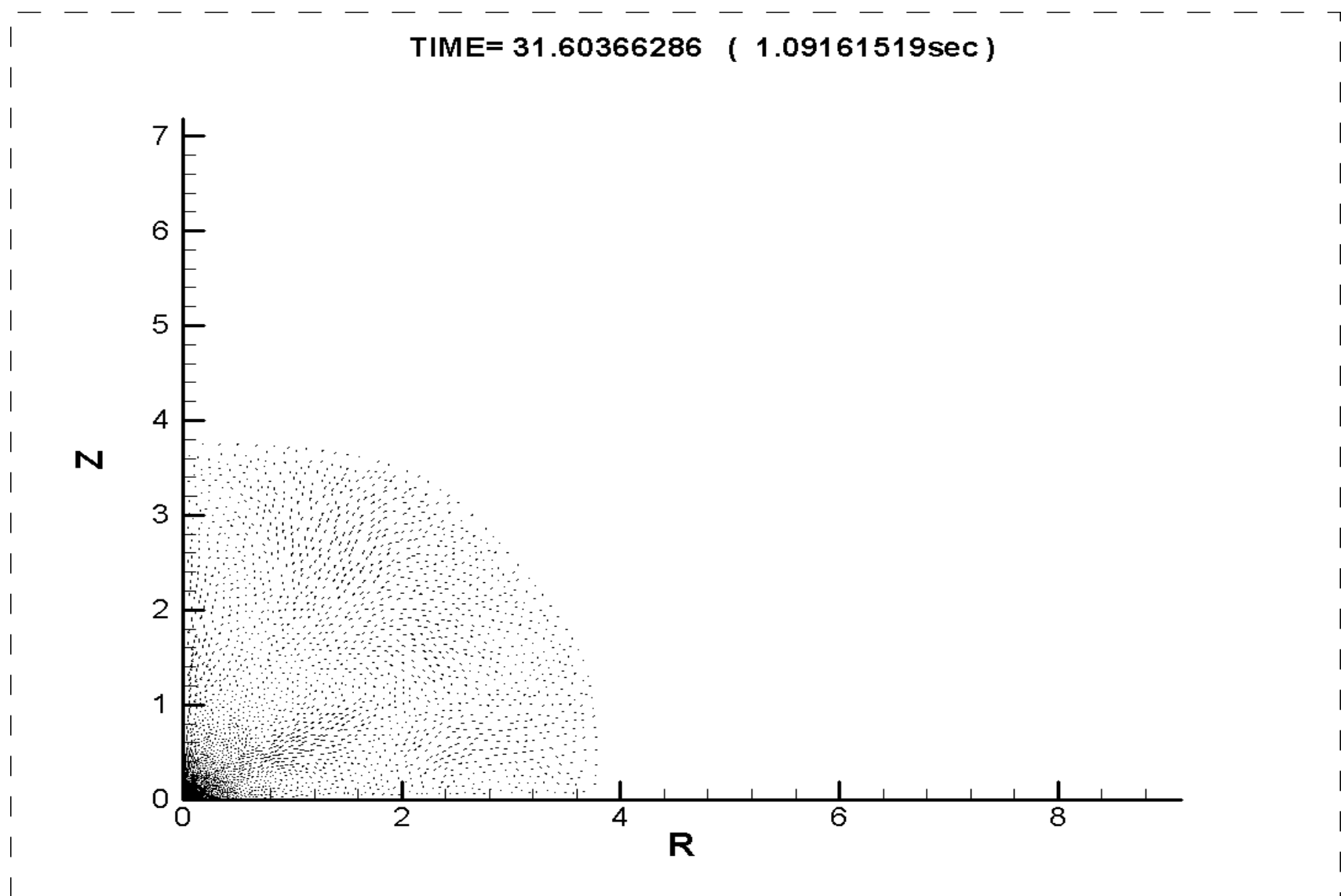


# Initial magnetic field – dipole-like symmetry

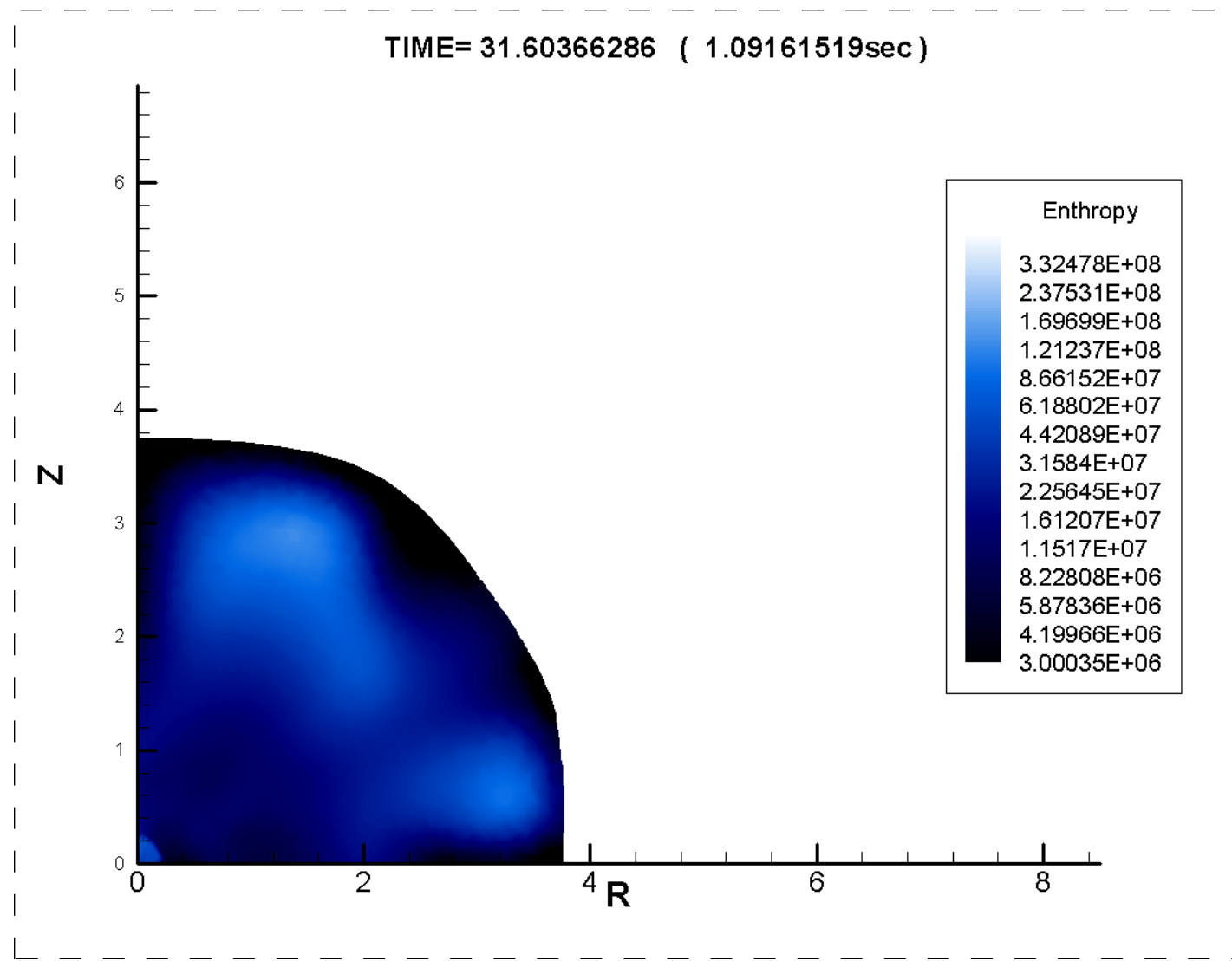
SM., Ardeljan & Bisnovatyi-Kogan MNRAS 2006, 370, 501



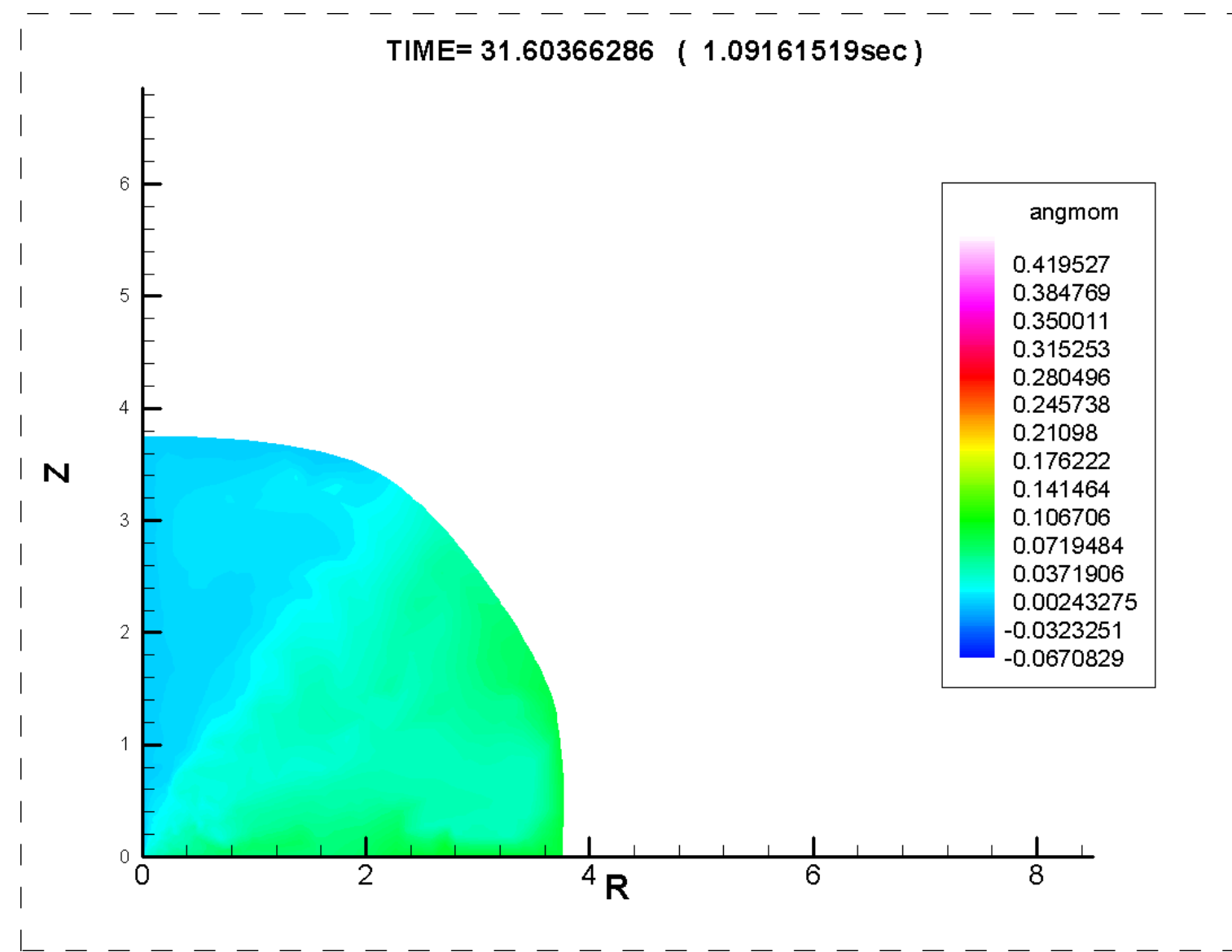
# Magnetorotational explosion for the **dipole-like** magnetic field



# Magnetorotational explosion for the **dipole-like** magnetic field



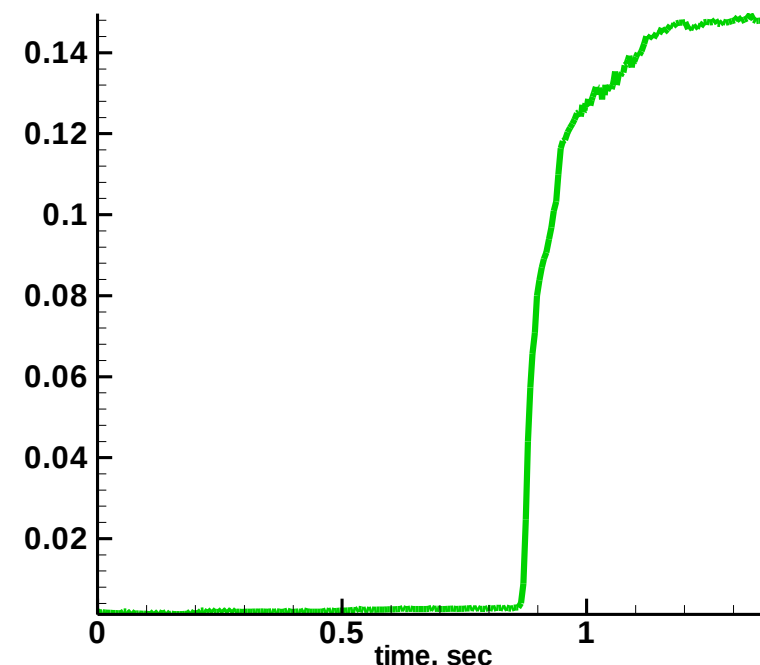
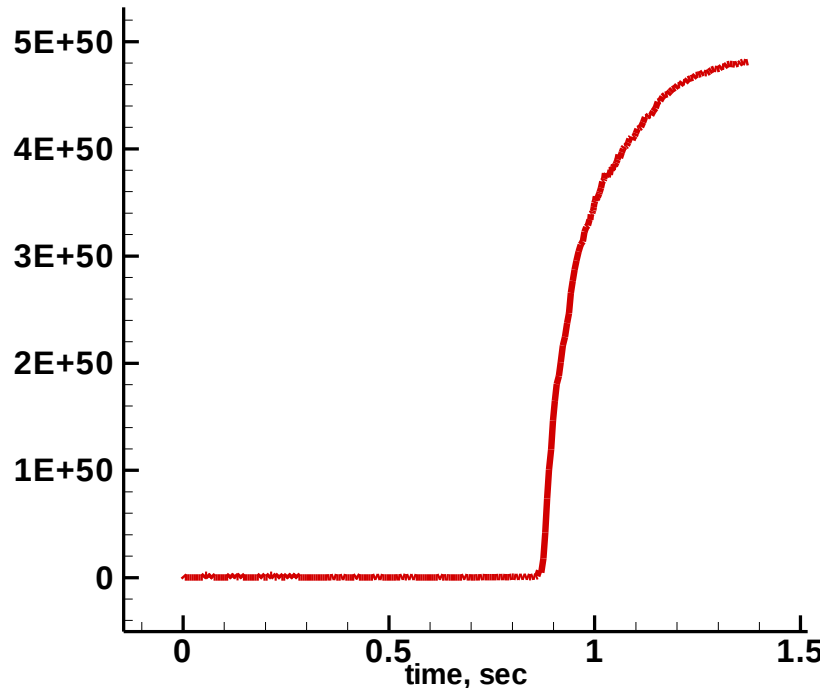
# Magnetorotational explosion for the **dipole-like** magnetic field



## Ejected energy and mass (dipole)

Ejected energy  $\approx 0.5 \times 10^{51} erg$       Ejected mass  $\approx 0.14 M_{\odot}$

Particle is considered “ejected” –  
if its kinetic energy is greater than its potential energy



# Characteristic time of the magnetic field reconnection (rough estimation)

Petcheck mechanism – characteristic reconnection time

$$\tau_{reconn} = \frac{4(\ln(Re_m) + 0.74)}{\pi v_A l^{-1}}$$

Our estimations show:  
conductivity  $\sim 8 \cdot 10^{20} \text{ C}^{-1}$   
Magnetic Reynolds number  $\sim 10^{15}$

Characteristic time of the magnetic field reconnection

For the magnetorotational supernova is:

$$\tau_{reconn} \approx 5 \text{ c}$$

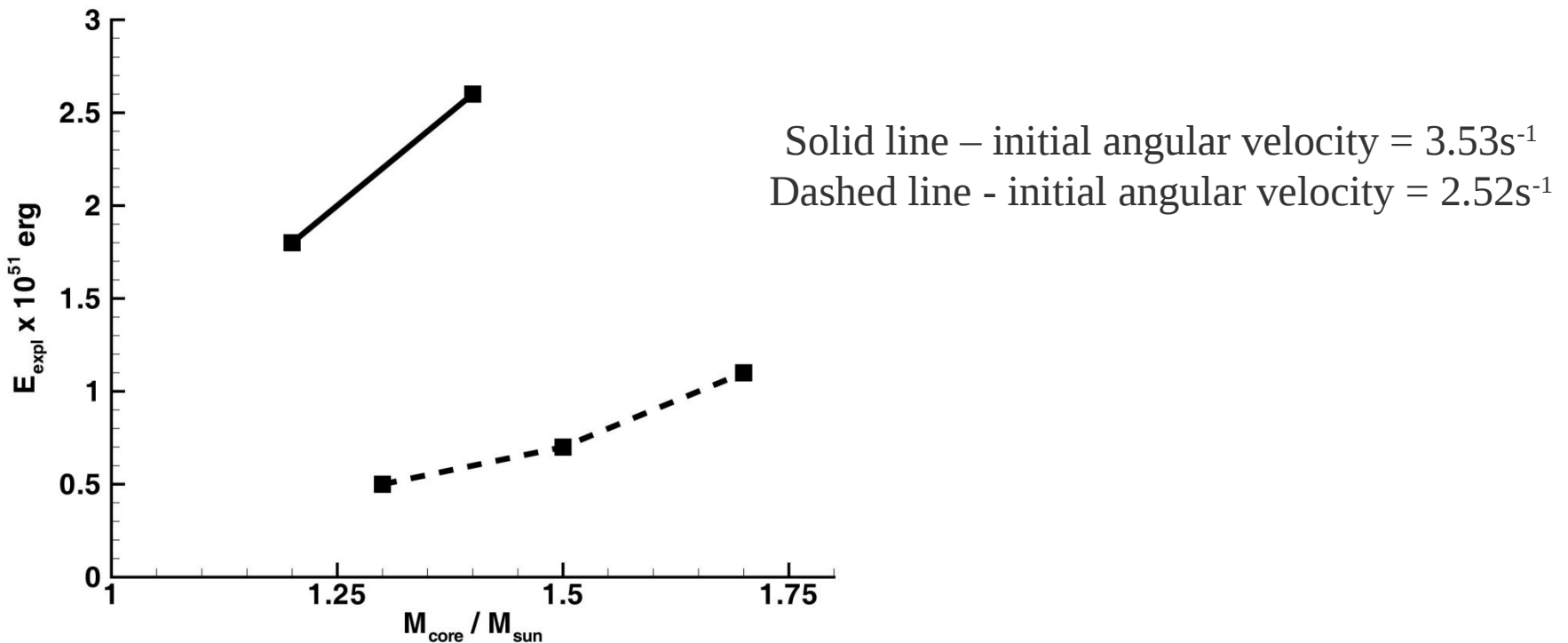
(approximately 10 times larger than  
characteristic time of magnetorotational  
supernova explosion).. .

Reconnection of the magnetic field does not influence  
significantly on the supernova explosion.

# MR supernova – different core masses

Bisnovatyi-Kogan, SM, 2008 (in preparation)

Dependence of the MR supernova explosion energy on the core mass and initial angular



The main difference of bounce shock and neutrino driven mechanisms from magnetorotational supernovae  magnetic field works like a piston. This **MHD piston supports the supernova MHD shock wave for some time.**

## 3D features of MR supernova simulations

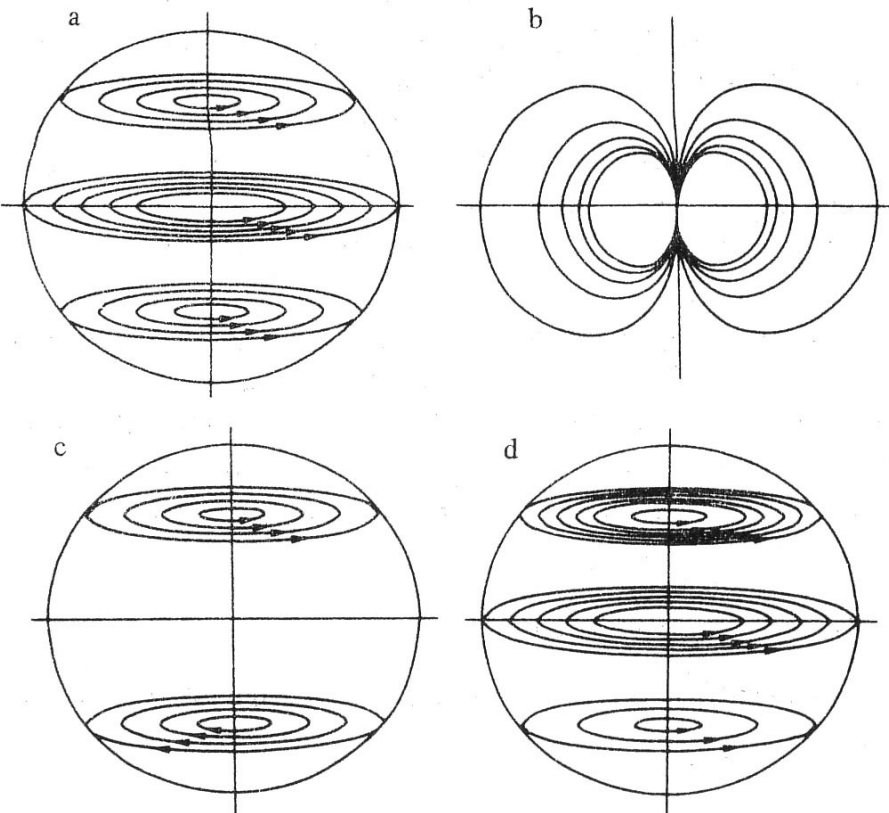
- Lagrangian grid (tetrahedrons) method requires frequent grid reconstruction near protoneutron star surface (due to differential rotation) => **violation of the solution**.
- Unstructured grid (Dirichlet cells) – construction of 3D grid of Dirichlet cells is **expensive**.
- SPH (Smooth Particle Hydrodynamics) – **poor spatial accuracy**, concentration of particles near gravitational center.

**Optimal :**

Eulerian scheme with Automatic Mesh Refinement : Approximate MHD Riemann solvers (problems with degeneration of eigenvectors and eigenvalues)  
Finite-difference schemes (e.g. central numerical schemes *Kurganov&Tadmor, Ziegler*).

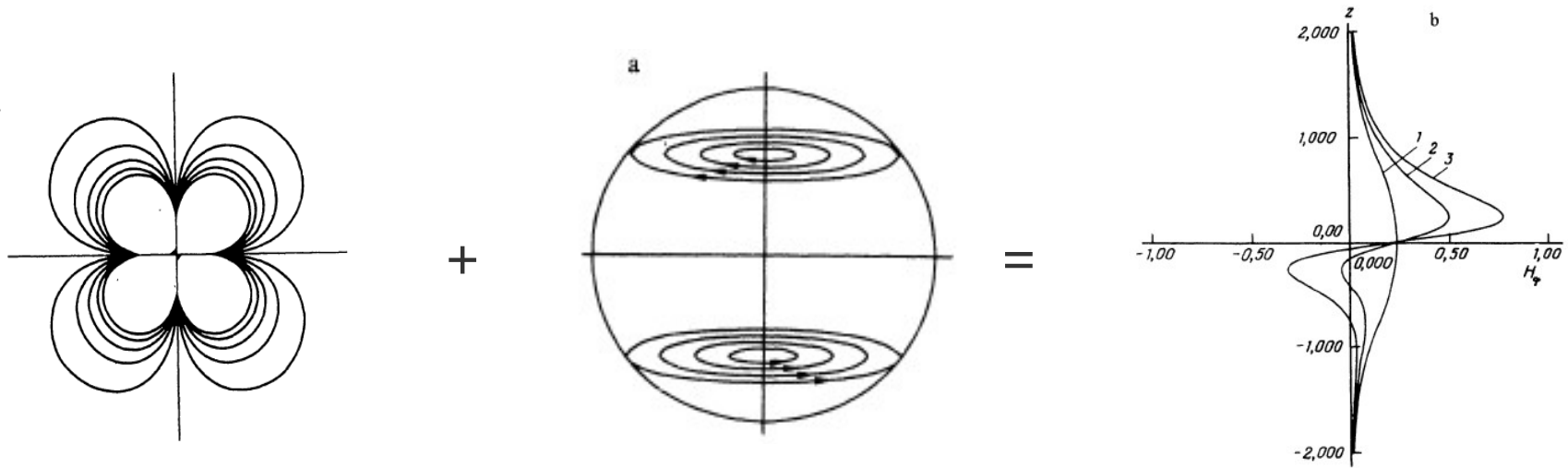
# Mirror symmetry violation of the magnetic field in rotating stars

Bisnovatyi-Kogan, S.M. Sov. Astr. 1992, 36, 285



- a. Initial toroidal field
- b. Initial dipole field
- c. Generated toroidal field
- d. Resulting toroidal field

# Mirror symmetry violation of the magnetic field in rotating stars



Resulting toroidal field is larger in the upper hemisphere.

**Violation of mirror symmetry of the magnetic field in magnetorotational explosion leads to:** One sided ejections along the rotational axis.

Rapidly moving radiopulsars (up to 300 km/s).

In reality we have dipole + quadrupole + other multipoles...

(Lovelace et al. 1992)

$$\text{Dipole} \sim \frac{1}{r^3}$$

$$\text{Quadrupole} \sim \frac{1}{r^4}$$

The magnetorotational supernova explosion is  
always  
asymmetrical.

For high magnetic fields neutrino cross-section depends on the magnetic field values.

(Bisnovatyi-Kogan, Astron. & Astroph. Trans., 1993, 3, 287, See also Lai, 1998)

The pulsar kick velocity can be up to 1000 km/s along rotational axis

Jet, kick and axis of rotation are aligned in MR supernovae.

# Evidence for alignment of the rotation and velocity vectors in pulsars

S. Johnston et al. MNRAS, 2005, 364, 1397

“We present strong observational evidence for a relationship between the direction of a pulsar's motion and its rotation axis. We show carefully calibrated polarization data for 25 pulsars, 20 of which display linearly polarized emission from the pulse longitude at closest approach to the magnetic pole...  
**we conclude that the velocity vector and the rotation axis are aligned at birth“.**

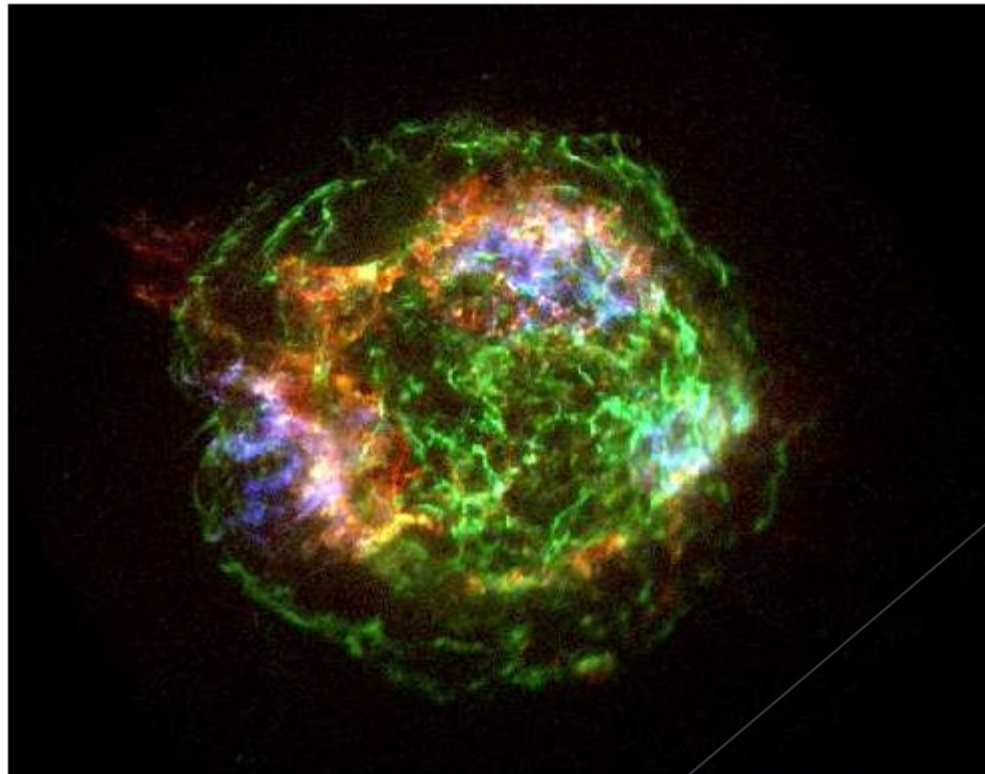
## Rapidly moving pulsar VLBI observations

W.H.T. Vlemmings et al. MmSAI, 2005, 76, 531

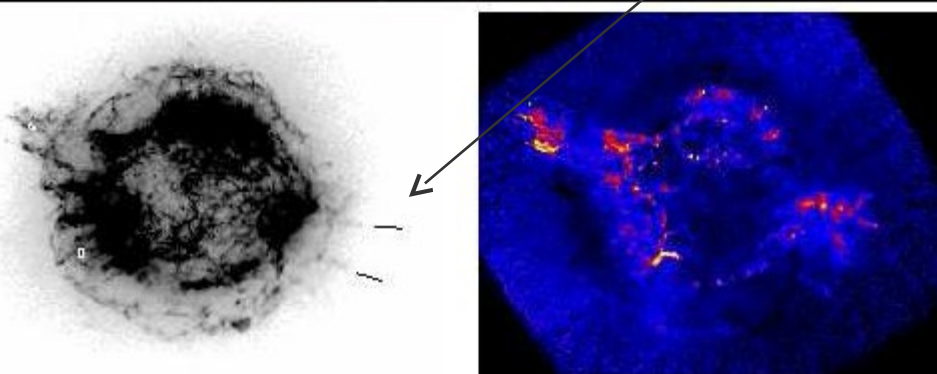
“Determination of pulsar parallaxes and proper motions addresses fundamental astrophysical questions. We have recently finished a VLBI astrometry project to determine the proper motions and parallaxes of 27 pulsars, thereby doubling the total number of pulsar parallaxes. Here we summarize our astrometric technique and present the ***discovery of a pulsar moving in excess of 1000 kms***, PSR B1508+55”.

# Cassiopea A- supernova with jets-an example of the magnetorotational supernova

(Hwang et al. ApJL, 2004, 615, L117 )



1 million Chandra survey of Cas A. Second jet was found.



# Conclusions

- Magnetorotational mechanism (MRM) produces enough energy for the core collapse supernova.
- The MRM is weakly sensitive to the neutrino cooling mechanism.
- MR supernova shape depends on the configuration of the magnetic field and is always asymmetrical.
- MRI develops in MR supernova explosion.
- One sided jets and rapidly moving pulsars can appear due to MR supernovae.
- 3D simulations of MR supernova are necessary.

Thank you!